Sensors and Actuators Reports 9 (2025) 100335

Contents lists available at ScienceDirect

Sensors and Actuators Reports

journal homepage: www.sciencedirect.com/journal/sensors-and-actuators-reports

Electrochemical genosensors on-a-chip: Applications in early diagnosis of pathogens

A. Dehghan [a], M.J. Kiani [a], A. Gholizadeh [a], J. Aminizadeh [b], A. Rahi [c,*], I. Zare [d], E. Pishbin [e,*], H. Heli [f,*]

[a] School of Mechanical Engineering, Iran University of Science and Technology, Tehran, Iran
[b] Center of Excellence in Energy Conversion (CEEC), School of Mechanical Engineering, Sharif University of Technology, Tehran, Iran
[c] Pathology and Stem cell Research Center, Kerman University of Medical Sciences, Kerman, Iran
[d] Research and Development Department, Sina Medical Biochemistry Technologies Co., Ltd., Shiraz 7178795844, Iran
[e] Bio-microfluidics Laboratory, Department of Electrical Engineering and Information Technology, Iranian Research Organization for Science and Technology, Tehran, Iran
[f] Nanomedicine and Nanobiology Research Center, Shiraz University of Medical Sciences, Shiraz, Iran

ARTICLE INFO

Keywords:
Electrochemical genosensors
Pathogen detection
Microfluidics
Nucleic acid biosensors
Point-of-care diagnostics

ABSTRACT

Electrochemical genosensors have emerged as a powerful tool for the early diagnosis of pathogens, offering advantages such as high sensitivity, rapid response times, low cost, and easy adaptability for point-of-care applications. This review highlights recent advancements in CRISPR-Cas-integrated electrochemical systems, novel nanomaterial architectures, and label-free detection mechanisms. Key innovations include anisotropic gold nanostructures, MXene composites with exceptional conductivity, and poly(ortho-aminophenol) films, which enable attomolar detection limits for pathogens such as bacteria and parasites. We evaluate DNA hybridization-based approaches, emphasizing innovations in signal amplification strategies such as saltatory rolling circle amplification and self-assembled monolayers, which address specificity challenges in complex matrices. Additionally, we highlight the integration of electrochemical genosensors with microfluidic platforms, including automated sample-to-answer workflows and multiplexed detection architectures, which address traditional laboratory bottlenecks. By cataloging advancements in material science, bioreceptor design, and microfluidic automation, this work provides a comprehensive yet focused resource for researchers advancing the frontiers of rapid, portable pathogen diagnostics. Furthermore, we explore the commercial potential of these technologies, providing insights that could guide the development of highly sensitive, field-deployable biosensors for clinical and environmental applications.

Abbreviations: (missDNA), Base mismatched DNA; (BSA), Bovine serum albumin; (*C. auris*), *Candida auris*; (E-CRISPR), Cas-integrated electrochemical; (CeO_2 NRs), Cerium oxide nanorods; (CS), Chitosan; (CRISPR), Clustered regularly interspaced short palindromic repeat; (cDNA), Complementary DNA; (CP), Conducting polymers; (Cas), CRISPR-associated; (DPV), Differential pulse voltammetry; (DSS), DNA super-sandwich; (dsDNA), Double-stranded DNA; (*E. faecalis*), *Enterococcus faecalis*; (EBV), Epstein-Barr Virus; (*E. coli*), *Escherichia coli*; (gDNA), Genomic DNA; (Au NPs), Gold nanoparticle; (Gr), Graphene; (HBV), Hepatitis B virus; (HRP), Horseradish peroxidase; (SA-HRP), HRP-labeled streptavidin; (EIS), Impedance spectroscopy; (LOC), Lab-on-a-chip; (*L. pneumophila*), *Legionella pneumophila*; *(L. infantum)*, *Leishmania infantum*; (*L. major*), *Leishmania major*; (LOD), Limit of detection; (LAMP), Loop-mediated isothermal amplification; (MP), Magnetic particle; (MB), Methylene blue; (*M. tuberculosis*), *Mycobacterium tuberculosis*; (NP), Nanoparticle; (ncDNA), Non-complementary DNA; (NA), Nucleic acid; (PNA), Peptide nucleic acid; (pPNA), Peptide nucleic acid probe; (POC), Point-of-care; (PANI), Poly(aniline); (PPy), Poly(pyrrole); (PCR), Polymerase chain reaction; (pDNA), Probe DNA; (RCA), Rolling circle amplification; (*Salmonella typhimuriumS. typhimurium*), *S.almonella typhimuriumalmonella Typhimurium*; (SRCA), Saltatory rolling circle amplification; (SPCE), Screen-printed carbon electrode; (SAM), Self-assembled monolayer; (ssDNA), Single-stranded DNA; (SWV), Square wave voltammetry; *(S. aureus)*, *Staphylococcus aureus*; (tDNA), Target DNA; (tDNA), Target ssDNA; (TB), Toluidine blue; (*T. vaginalis*), *Trichomonas vaginalis*.

* Corresponding authors.
E-mail addresses: amidrahi@gmail.com (A. Rahi), es.pishbin@gmil.com (E. Pishbin), heli@sums.ac.ir (H. Heli).

https://doi.org/10.1016/j.snr.2025.100335
Received 14 December 2024; Received in revised form 30 April 2025; Accepted 5 May 2025
Available online 6 May 2025

1. Introduction

The latest global health crisis, COVID-19, has once again substantiated the reality that infectious diseases continue to pose a primary challenge in healthcare systems worldwide in spite of significant progress in the medical sciences. Approximately 15 % of global mortality is believed to result from infectious diseases [1]. Pathogens of viruses, bacteria, fungi, and protozoa are major causes of widespread diseases, and among these, viruses and bacteria are the most prevalent. The development of sensitive, rapid, and field-applicable techniques for detecting these pathogens is crucial to prompt diagnosis and treatment of infectious diseases to prevent their spread and global impact on human health [2].

Innovative methods have emerged through discoveries such as new biomarkers, utilization of new technologies such as nanotechnology, and advances in microfluidic-based miniaturization, allowing for the development of portable, accurate, rapid, and cost-effective point-of-care (POC) detection platforms. Molecular diagnostics employing DNA and RNA biomarkers represent the forefront of detection mechanisms for infectious diseases. Despite the considerable sensitivities offered by conventional techniques relying on antibodies, such as enzyme-linked immunosorbent assay and polymerase chain reaction (PCR), they suffer from drawbacks including being time-consuming, labor-intensive, and reliant on relatively expensive equipment. Additionally, their applicability is constrained to laboratory settings due to the necessity for sample pre-treatment [2].

Biosensors, particularly electrochemical genosensors, have gained prominence as diagnostic tools due to their rapidity, specificity, and adaptability. Over the past 50 years, they have revolutionized healthcare by enabling early diseases detection. Their efficacy in clinical care, coupled with attributes such as rapidity, specificity, and responsiveness, is deemed crucial for enabling early diagnosis and treatment [3]. The integration of transducers into biomaterials has facilitated the creation of interfaces capable of generating signals, appropriately referred to as biosensors. Biosensors may be categorized according to the structure of the transducer, labeling, and general configuration, tailored to specific functionalities and affinities. The recognition of analytes frequently induces a change in the three-dimensional structure, which is then transduced into a signal [4]. Biosensors are broadly classified based on their signal transduction mechanisms, including optical (emission, absorption, surface plasmon resonance), piezoelectric (mass-sensitive quartz crystal microbalance), thermal, and electrochemical biosensors [5]. While optical biosensors offer high sensitivity, they often require complex instrumentation and are less portable. Piezoelectric and thermal biosensors, though label-free, suffer from limited multiplexing capabilities and slower response times. While, electrochemical biosensors have gained significant attention due to their high sensitivity, cost-effectiveness, and rapid response times [6].

Electrochemical biosensors, particularly electrochemical genosensors, offer distinct advantages, including low power consumption, compatibility with microfluidic platforms, and real-time signal transduction. These genosensors operate by detecting nucleic acid (NA) hybridization events via electrochemical readout, eliminating the need for bulky optical detection systems. At their core, electrochemical genosensors consist of a biological sensing system and an electrochemical transducer with a primary focus on detecting present or prospective alterations associated with interactions that occur at the sensor/sample interface [7]. Regarding the electrochemical genosensors, a fundamental analytical factor in determining DNA hybridization that should be given paramount significance is the electrochemical response alteration in the target DNA (tDNA) absence and presence. Enhancing sensitivity and lowering the limit of detection (LOD) pose the primary hurdles in the advancement of electrochemical biosensors to detect minute amounts of analyte in real samples. To overcome these problems, nanomaterials, due to their unique physicochemical properties, are regarded as next-generation electrochemical biosensors. Different nanomaterials are used in electrochemical biosensors fabrication, including metallic nanostructures of gold [8], palladium [9] and silver [10], metal oxide nanostructures [11], semiconductors [12] and carbon allotropes [13], which are the most stable nanoparticles (NPs) with high potential in the fields of biosensing and diagnostics because of their exceptional optical, chemical, and electrical properties.

The extensively miniaturized microfluidic technology enables the integration of intricate NA detection procedures on a single chip [14, 15], which simplifies the procedures and contributes to the establishment of automated and effective diagnostic systems [16–19]. The integration of microfluidics with NA hybridization detection can also enhance the sensitivity of the assay, rendering it a potent instrument for clinical microbiology examinations and amplified signal generation for analysis of minimal amounts of DNA and RNA [20–23]. Integration of electrochemical genosensors with analytical microfluidic devices as a single miniaturized platform is a promising approach that has already been explored in both research and certain commercial biomedical products [24]. The combination of these two platforms offers benefits in contrast to conventional electrochemical sensing systems, such as accurate manipulation of small sample quantities, disposability, need for a reduced number of samples, cost efficiency, and rapid analysis. The capability to operate with a small sample size enables improved detection sensitivity while reducing operator exposure to harmful pathogens [25,26]. Most importantly, this integration also introduces the multiplexing mode, such as the concurrent detection of various target species within a singular sample, thereby addressing traditional laboratory bottlenecks through automated workflows [2].

In this review, we provide a comprehensive analysis of recent advancements in electrochemical genosensors for pathogen detection (Scheme 1). We begin by discussing various electrochemical genosensing approaches, highlighting DNA hybridization-based techniques, signal amplification strategies, and the role of self-assembled monolayers. Next, we explore the integration of nanomaterials, including metallic nanostructures and conducting polymers, in enhancing the sensitivity and selectivity of genosensors. We then examine the emerging role of CRISPR-powered electrochemical genosensors and their impact on attomolar-level detection. Further, we discuss the integration of NA amplification techniques, such as loop-mediated isothermal amplification, with electrochemical detection to improve diagnostic accuracy. We also cover applications of electrochemical genosensors for bacterial, viral, fungal, and parasitic pathogen detection, providing examples of recent innovations. Finally, we highlight the convergence of electrochemical genosensors with microfluidics for automated, high-throughput detection and discuss commercialization prospects, addressing challenges and future directions in the field. By structuring this review in a focused manner, we aim to provide a valuable resource for researchers developing next-generation pathogen detection technologies.

2. Electrochemical genosensing approaches

NA-based biosensors rely on sequence-specific base pairing between probe DNA (pDNA) and tDNA. For example, DNA microarrays enable semi-quantitative and multiplexed gene expression analysis in a single assay [27]. Typically, these biosensors employ a single-stranded DNA (ssDNA; pDNA) immobilized on a transducer surface. When this pDNA recognizes and hybridizes with its tDNA or complementary (target) RNA, electrochemical techniques facilitate signal transduction, while variations exist on the fundamentals of pDNA/tDNA interactions. One approach utilizes peptide nucleic acid (PNA) probes (pPNAs), where the negatively charged DNA sugar-phosphate backbone is substituted with a neutral pseudopeptide chain. pPNAs exhibit enhanced binding affinities (compared to their ssDNA counterparts) for tDNA, and the decreased charge on these pPNAs offers advantages for certain electroanalytical methods. Another variation is the sandwich assay, wherein an immobilized probe binds to one region of an analyte, while a labeled probe

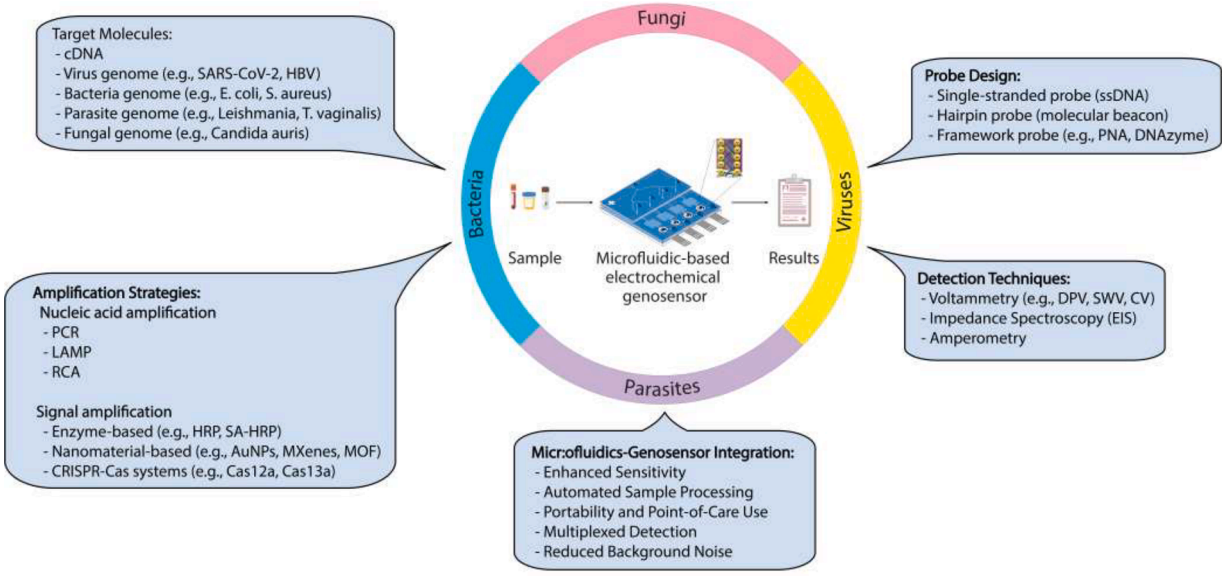

Scheme 1. Recent advancements in electrochemical genosensors for pathogen detection.

binds to a different region. A third variation, termed ''molecular beacon'', involves probe sequences that self-bind to form stem-and-loop or hairpin structures. tDNAs compete for binding with these structures, inducing a conformational change in the probe and enabling highly sensitive detection of low tDNA quantities. The most effective NA biosensors can discern between tDNA and one with a single base mismatched DNA (missDNA), a level of specificity necessary for identifying single nucleotide polymorphisms. There is significant interest in employing single nucleotide polymorphism detection to identify patients with genetic disorders. Having explored the fundamental electrochemical genosensing approaches, it is essential to consider how the immobilization of NAs on sensor surfaces plays a crucial role in enhancing detection performance. In the following section, we examine the role of self-assembled monolayers (SAMs) in optimizing hybridization efficiency and signal transduction.

3. NA self-assembled monolayers (SAMs)

Immobilized pDNA orientation on electrode surfaces critically influences electrochemical performance and hybridization efficiency. While ssDNA with a persistence length of ~1 nm is highly flexible and demonstrates a temperature-dependent behavior, double-stranded DNA (dsDNA) is more resilient, exhibits a rod-like shape, and is characterized by a persistence length of up to 50 nm. Beyond DNA and RNA, various other NA structures such as PNAs hold an appeal for the advancement of biosensors. Most current NA detection approaches rely on the hybridization process between pDNA and tDNA, and (unless hybridization occurs in a solution) its effectiveness is heavily reliant on the accessibility of pDNA for hybridization and, consequently, on the pDNA immobilization technique employed. The most straightforward immobilization method involves the physical adsorption of pDNA onto electrode surfaces, resulting in biomolecules lying flat on the surface [28]. This state allows for DNA analysis either through its direct electrochemical oxidation/reduction or by monitoring signals from redox indicators. To exert more precise control over the pDNA surface state, electrostatic interactions between the sugar-phosphate backbone of pDNA and positively charged surfaces, such as poly(ethyleneimine)-modified surface or amino-silanized glass, have been employed to create functional DNA electrodes capable of highly specific hybridization reactions [29]. More intricate immobilization methods involve attaching pDNA to the surfaces using synthetic linkers introduced through automated NA synthesis, either at the 5′ or 3′ end of the DNA sequence [30]. This arrangement aims to orient the DNA molecule toward the solution phase, making it more accessible for hybridization. On gold and some other metallic electrode surfaces such as silver and platinum, pDNA can be immobilized using alkanethiol linkers, cyclic disulfides, and multiple dithiol tags [31–33]. Since ssDNA is strongly chemisorbed on the gold surface via its structural bases, the gold surface must be additionally blocked by alkanethiols such as 6-mercapto-1-hexanol to prevent nonspecific adsorption of pDNA. A dual back-filler comprising 6-mercapto-1-hexanol and dithiothreitol co-adsorbed with pDNA creates a highly compact ternary monolayer with lower background noise and increased resistance to fouling [34–36]. Less commonly employed are strategies involving the covalent attachment of unmodified pDNAs to functionalized alkanethiol SAMs. For instance, this can be achieved through carbodiimide coupling between the -COOH-terminated SAM and the 3′-hydroxy end of DNA [37] although this approach results in a less controlled composition of the produced pDNA layers. While SAMs provide a stable and well-organized interface for DNA immobilization, additional strategies are needed to further improve sensor sensitivity and stability. Conducting and non-conducting polymers offer versatile platforms for DNA immobilization and signal amplification, as discussed in the next section.

4. Conducting and non-conducting polymer-based electrochemical genosensors

Conducting polymers (CPs), such as poly(aniline) (PANI) and poly (pyrrole) (PPy) are cost-effective and tunable materials widely used in electrochemical biosensors. Their high conductivity and biocompatibility make them ideal for biomolecule immobilization. The selectivity, sensitivity, stability, and reproducibility of the electrochemical biosensors' responses can be improved by designing CPs through chemical grafting of functional groups, nanostructures, or combining them with NPs [38–40]. The most popular CPs that have been developed so far are poly(aniline) (PANI), poly(2-aminophenol), poly(4-aminophenol), poly (3,4-ethylenedioxythiophene), poly(pyrrole) (PPy), poly(thiophene), and poly(5-carboxyindole) [41–45]. In an investigation, gold NPs (Au NPs) were utilized with PANI in an electrochemical sensing platform for the fast detection of *Escherichia coli* (*E. coli*) [46]. This biosensor was designed based on a dual-signal amplified strategy and a screen-printed carbon electrode (SPCE) modified with PANI and Au NPs as substrates. Then, the biotinylated pDNA was immobilized on the PANI/Au NP/avidin composite on the SPCE surface via biotin-avidin interaction.

Subsequently, a hybridization solution containing bacterial lysis, a digoxigenin-labeled pDNA, and an anti-digoxigenin-labeled horseradish peroxidase (HRP) enzyme was added to the SPCE surface. Finally, tetramethylbenzidine was placed on the electrode surface, and the cyclic voltammetry measurement was employed for detection (Fig. 1A). The proposed genosensor can detect as low as 4 CFU mL^{-1} of *E. coli* bacteria and had a linear detection range of 4 to 4×10^6 CFU mL^{-1}. This biosensing system was able to rapidly detect *E. coli* in urine and water samples.

In another study, a label-free DNA sensor was developed using a composite of cerium oxide nanorods (CeO_2 NRs) decorated with PPy NPs for the detection of *Salmonella* [47]. The incorporation of PPy NPs into CeO_2 NRs enhanced the conductivity and stability of the electrode, optimizing it for electrochemical applications. The sensor was fabricated through the hydrothermal synthesis of CeO_2-NRs, followed by in-situ chemical oxidative polymerization of pyrrole, resulting in a composite electrode that allowed for the covalent immobilization of ssDNA sequences (Fig. 1B). The electrochemical performance of the sensor was assessed using electrochemical impedance spectroscopy (EIS) with $[Fe(CN)_6]^{3-/4-}$ as a redox marker, exhibiting a linear response for DNA detection over a concentration range of 1.0×10^{-9} to 1.0×10^{-6} mol L^{-1}. The sensor demonstrated a LOD of 2.86×10^{-7} mol L^{-1}. This study reinforces the significant performance enhancements electrochemical sensors gained from combining CPs like PPy with nanostructured materials.

Khoder et al. investigated the potential of a nanostructured PPy formed through template-free electrochemical polymerization, as an effective platform for amperometric DNA detection [48]. To enhance functionality, the PPy surface was aminated through the electrochemical oxidation of ethylenediamine or poly(amidoamine) dendrimers, enabling the covalent attachment of pDNAs and ferrocene redox reporters. The resulting modified PPy exhibited key properties such as high surface area, hydrophilicity, and rapid electron transfer rates (up to 18 s^{-1}), contributing to improved DNA sensing performance. The biosensor demonstrated a detection limit of 0.36 atomolar without requiring amplification and successfully identified genomic DNA (gDNA) of *Mycobacterium tuberculosis* (*M. tuberculosis*), distinguishing between wild-type and mutant strains with high specificity (Fig. 1C).

On the other hand, non-conductive polymers play a pivotal role in advancing electrochemical biosensors by minimizing background signals due to their insulating nature. This property significantly enhances the specificity and sensitivity of genosensors. Among these polymers, chitosan (CS), a naturally derived material, has gained a lot of attention. With its rich amine groups, CS enables the covalent attachment of various biomolecules, making it a versatile substrate for sensor development [49]. In the realm of DNA-based biosensors, researchers commonly used CS as a platform for immobilizing pDNA modified with an amine group, facilitated by the linker glutaraldehyde [50,51]. Notably, its non-conductive nature hasn't limited its applications; on the contrary, researchers have successfully combined CS with various conductive 0-to-2D materials to enhance electrical conductivity and, consequently, the sensitivity of detection [52–54]. This integration showcases the adaptability of CS to optimize the performance of electrochemical genosensors (Table 1). For instance, Wasiewska et al. [8] developed a highly sensitive electrochemical genosensor for the determination of Shiga toxin-producing *E. coli* by targeting the stx1 gene using Au NPs and CS nanocomposite to immobilize a pDNA through covalent bonding (Fig. 2A).

In another investigation, CS was employed in the development of electronic tongues and genosensors for pathogen detection, such as *Staphylococcus aureus (S. aureus)* DNA, a significant pathogen in bovine mastitis [55]. CS was utilized to create layer-by-layer films on microfluidic interdigitated electrodes. The genosensors, comprising 10 bilayers of CS/chondroitin sulfate or 8 bilayers of CS/sericin, were functionalized with an active layer of pDNA *S. aureus* and demonstrated high sensitivity with a detection limit of 5.90×10^{-19} mol L^{-1} through specific DNA hybridization. The performance of both sensor types was enhanced by machine learning techniques, achieving an accuracy of up to 89 % for genosensing. The use of CS allows for potential applications in wearable devices due to their biocompatibility and low-cost nature.

Further demonstrating the versatility of CS, another study developed an electrochemical genosensor using a composite of multiwalled carbon nanotubes, CS, and bismuth, combined with lead sulfide NPs as a signaling pDNA (Fig. 2B) [56]. This sensor achieved a detection limit of 1.0×10^{-14} mol L^{-1} for pathogenic *Aeromonas* species. The role of CS in this sensor is pivotal, contributing to its biocompatibility, mechanical strength, and excellent film-forming ability. The sensor demonstrated a significant potential for applications in biomedical diagnostics, food safety, and environmental monitoring.

In another study, an electrochemical genosensor was developed, using a hybrid nanocomposite of iron oxide and CS modified with graphene (Gr) oxide [57]. The properties of CS enhanced the sensor's electrochemical performance by providing a suitable environment for pDNA immobilization due to its excellent film-forming ability and nontoxicity. The hybrid nanocomposite was synthesized and deposited onto an indium tin oxide electrode, where it facilitates the covalent attachment of specific pDNAs targeting *E. coli* DNA (Fig. 2C). EIS revealed a linear response to complementary DNA (cDNA) concentrations from 10^{-6} to 10^{-14} mol L^{-1}, with a detection limit of 1.0×10^{-14} mol L^{-1}. The inclusion of CS not only improves the sensor's mechanical strength, but also enhances the electrochemical properties by increasing the effective surface area for DNA immobilization.

5. MXenes and metal-organic frameworks (MOFs) for genosensing

MXenes, a class of two-dimensional transition metal carbides/nitrides, have emerged as transformative materials for electrochemical genosensing due to their high conductivity, hydrophilic surfaces, tunable surface chemistry, and exceptional mechanical stability. These properties lead to enhance signal-to-noise ratio. The terminal hydroxyl/oxygen groups on MXenes enable covalent functionalization of pDNAs with minimizing nonspecific adsorption in complex biological matrices, while their high surface area enhances charge transfer and stabilizes nanocomposite interfaces. These properties position MXenes as ideal substrates for sensitive and selective NA detection [58]. Metal-organic frameworks (MOFs), crystalline porous materials with ultrahigh surface areas, tunable pore sizes, and functionalizable ligands, further expand the nanomaterial toolkit. MOFs' modular architectures allow for pDNA immobilization within their cavities, while their porosity facilitates target preconcentration and localized signal amplification [13].

Ketabi et al. introduced an electrochemical genosensor for rotavirus RNA detection, leveraging a nanocomposite of hierarchical flower-like gold nanostructures, MXene, and PPy [59]. MXene nanosheets were synergized with PPy to amplify electrochemical signals. The MXene/PPy composite provided a stable platform for anchoring thiolated ssDNA probes, while its high surface area enhanced electron transfer kinetics. This design achieved a detection limit of 0.8×10^{-18} mol L^{-1} across a broad range (10^{-18}–10^{-7} mol L^{-1}) and maintained 95.1 % performance over 24 days, underscoring MXenes' role in improving both sensitivity and long-term stability. Building on MXenes' versatility, a biosensor for *M. tuberculosis* using Ti_3C_2 MXenes functionalized with zirconium ions was developed [60]. The zirconium-modified MXenes selectively bound to phosphate groups on 16S rDNA fragments, bridging nanogap electrodes to alter conductance. This interaction eliminated the need for probes, streamlining detection to 2 h with a LOD of 20 CFU mL^{-1}. MXenes' conductivity and surface chemistry enabled rapid, specific identification in sputum samples, highlighting their utility in resource-limited settings. MOFs have unlocked new possibilities through their porous structures and design flexibility. Cerium-based MOFs (Ce-MOF) with dendritic palladium nanostructures and sulfur-doped graphene oxide for SARS-CoV-2 detection [61]. The Ce-MOF's high

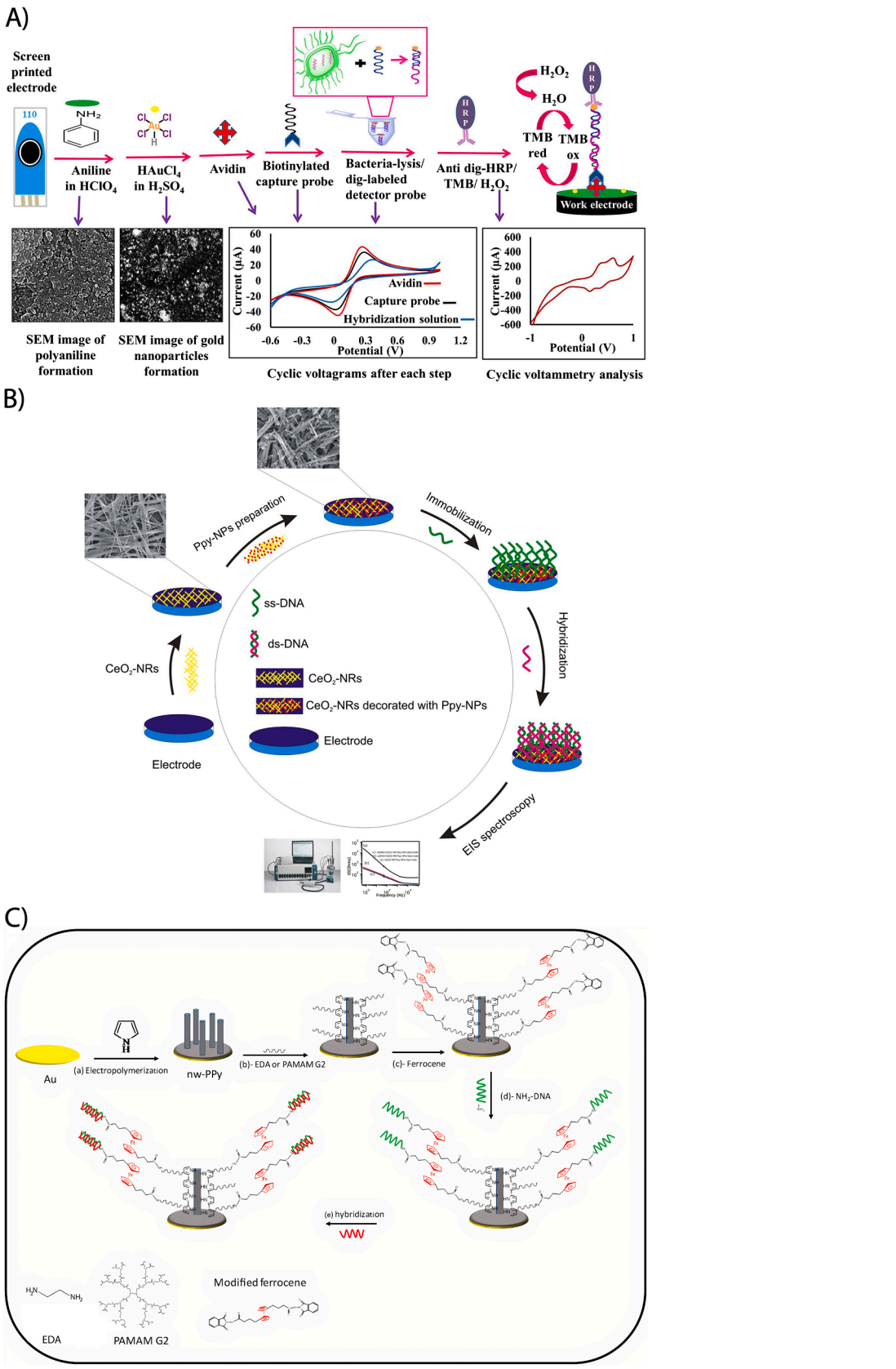

Fig. 1. A) Schematic presentation of a voltammetric DNA recognition strategy for *E. coli* using an electrode modified with PANI and Au NPs. TMB denoted 3,3′,5,5′-tetramethylbenzidine. Adapted with permission from [46]. Copyright 2019, Springer Nature. B) Schematic presentation of a DNA biosensor for *Salmonella* based on CeO_2 NRs decorated with PPy NPs. Adapted with permission from [47]. Copyright 2019, Springer Nature. C) Schematic presentation of a DNA biosensor for *M. tuberculosis* based on PPy nanowires (nw-PPy). PAMAM G2 denotes polyamidoamine of second generation. Adapted with permission from [48]. Copyright 2020, Elsevier.

Table 1
Electrochemical genosensors for detection of pathogens.

Analyte	Electrode	pDNA sequence	Nanomaterial (s)	Detection technique	Detection range	LOD	Ref.
stx1 gene of Shiga toxin-producing *E. coli*	Interdigitated Au	5′-CTGGATGATCTCAGTGGGCGTTCTTATGTAA-3′	Au NPs and a CS-Au nanocomposite	SWV	10^{-16} to 10^{-6} mol L^{-1}	100 amol L^{-1}	[8]
E. coli	SPCE	5′-GTCAATGAGCAAAGGTATTAACTTTACTCCCTTCC-3′	PANI and Au NPs	CV	4×10^{6}–4 CFU	4 CFU	[46]
Salmonella	N/A	5′-GGCTGGTACCACCTCTTCTACCATGG-3′	CeO_2 NRs, and Ppy NPs	EIS	1.0×10^{-9}–1.0×10^{-6} mol L^{-1}	2.86×10^{-7} mol L^{-1}	[47]
M. Tuberculosis	Au	5′-CCGACTGTTGGCGCTGGG-3′	PPy nanowires	Amperometry	1 amol L^{-1}–1 pmol L^{-1}	0.36 amol L^{-1}	[48]
S. aureus	Interdigitated Au	5′-GGACGACATTAGACGAATCA-3′	CS, chondroitin sulphate, sericin and Au NPs modified with sericin	EIS	1×10^{-18}–1×10^{-6} mol L^{-1}	5.90×10^{-19} mol L^{-1}	[55]
Aeromonas	Glassy carbon	N/A	MWCNTs, CS, Bi, and PbS NPs	DPV	3×10^{-13}–1.1×10^{-14} mol L^{-1}	1×10^{-14} mol L^{-1}, $>10^{2}$ CFU mL^{-1} of *Aeromonas*	[56]
E. coli	In-Sn oxide	5′-GGTCCGCTTGCTCTCGC-3′	Gr oxide, iron oxide NPs, and CS	EIS	10^{-6}-10^{-14} mol L^{-1}	1×10^{-14} mol L^{-1}	[57]
S. aureus	Glassy carbon	5'-TTATTTTATTTTATT-3'	Au NPs	SWV	0.415 fg μL^{-1}–41.5 ng μL^{-1}	2.51 fg μL^{-1}	[62]
S. Typhimurium	Au	5′-TCAGCGTTCCTTTACCATTTTTTTAACTTATTTGGTTTTTTTTTT-3′	N/A	DPV	6.7×10^{1}–6.7×10^{5} CFU mL^{-1}	55 CFU mL^{-1}	[63]
Salmonella	In-Sn oxide	Capture probe: 5′-CCGTTCTGACGCTGGCCCACTTCA-3′ Signaling probe: 5′-CCGGACGAATATCGTCGTAATGGCTGAAGGTGGAGTACA-3′	N/A	DPV	1 to 1000 genome units	2.4 nmol L^{-1}	[69]
Corynebacterium diphtheriae	Au	5′-AGGAATCGAAAACTTTTCTTCGTACCACGGGACTAAACCTGGTTATGTAGATTCC-3′	N/A	SWV	After 5 min hybridization: 0.16-2 μmol L^{-1} After 30 min hybridization: 13.5-60 nmol L^{-1}	After 5 min hybridization: 20.8 nmol L^{-1} After 30 min hybridization: 0.5 nmol L^{-1}	[73]
Salmonella	Glassy carbon	5′-TTT TTG ATG AGT-3′	PPy-rGO and Au NPs	DPV	For synthetic tDNA: 1.0×10^{-16}–1.0×10^{-10} mol L^{-1} For *Salmonella*: 9.6-9.6×10^{4} CFU mL^{-1}	For synthetic tDNA: 4.7×10^{-17} mol L^{-1} For *Salmonella*: 8.07 CFU mL^{-1}	[74]
M. Tuberculosis	Screen-printed Gr	5′-GCCCCGATGGTTTGCG-3′ 5′-GGGTTAGCCACACTTTGCG-3′ 5′-TAGGTCGATGGGGCGATCGG/TTTT/GGGTGTCGAGTCGATCTGC-3′ 5′-GCGCGATGGCGAACTCAAGG/TTTT/GGCACCGTAAACACCGTAG-3′ 5′-CAGCTCGGTCAGCTGTGT-3′ 5′-CACATCAGCCGCGTCCA-3′	Gr NPs	CV	N/A	1 pg total DNA, 40 genome equivalents of *M. Tuberculosis*	[70]
E. coli	SPCE	5′-GTTACCCGCAGAAGAAGAGTGTACCGACCTCAGTATCTTGCGACGTCAGTGGATAGTGTCTTACACGATTTATACCTTTGCTCATTGAC-3′	Streptavidin MPs	SWV	N/A	6.7 amol	[76]

Additional abbreviations:
Cyclic voltammetry (CV).
Multi-walled carbon nanotubes (MWCNTs).
Reduced graphene oxide (rGrO).
Square wave voltammetry (SWV).

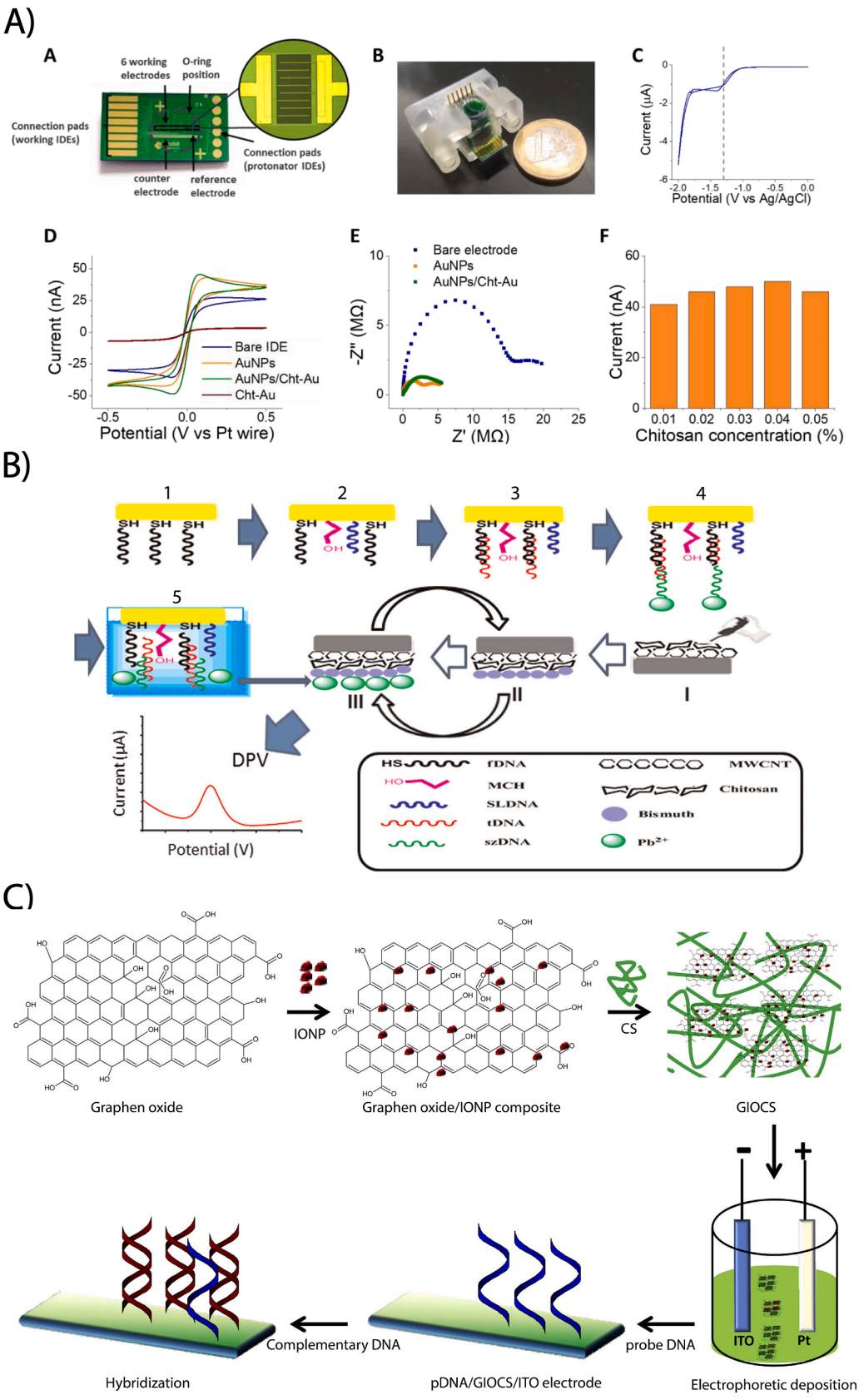

(caption on next page)

Fig. 2. A) A fully integrated silicon chip and an optical image of interdigitated gold microelectrode (IDE) (A), silicon chip in a chip holder (B), cyclic voltammograms recorded using an IDE-based sensor in 0.04 % CS, 50 ppm Au pH 5 (C), cyclic voltammograms in 5 mmol L^{-1} $Fe(CN)_6^{3-}/Fe(CN)_6^{4-}$, 0.1 mol L^{-1} KCl at (i) unmodified IDE and after deposition of (ii) 0.4 % CS with 50 ppm $HAuCl_4$ (Cht-Au), (iii) Au NPs, and (iv) Au NPs/Cht-Au (D), impedance measurements in 5 mmol L^{-1} $Fe(CN)_6^{3-}/Fe(CN)_6^{4-}$, 0.1 mol L^{-1} KCl at (i) unmodified IDE and after deposition of (ii) Au NPs and (iii) Au NPs/Cht-Au (E), and oxidation peak current of 5 mmol L^{-1} $Fe(CN)_6^{3-}/Fe(CN)_6^{4-}$, 0.1 mol L^{-1} KCl at IDE modified with ChtAu nanocomposite where the concentration of CS varied between 0.01 and 0.05 %. Adapted without needing permission from [8]. Copyright 2022, Elsevier. B) Schematic representation of an electrochemical genosensor using a composite of multiwalled carbon nanotubes, CS, and Bi, combined with PbS NPs as a signaling pDNA. 1–5: hybridization steps and dissolution of sandwich structure in 1 mol L^{-1} HNO_3. I-III: decoration of a glassy carbon with multiwalled carbon nanotubes-CC-Bi and electrodeposition of Pb^{2+}. Adapted with permission from [56]. Copyright 2015, Elsevier. C) Schematic representation of preparation of a hybrid nanocomposite of iron oxide and CS modified with Gr oxide on the surface of an In-Sn oxide surface, and its application for electrochemical detection of *E. coli*. Adapted with permission from [57]. Copyright 2015, Elsevier.

surface area and coordinatively unsaturated cerium sites optimized DNA probe loading and catalytic activity, yielding a LOD of 0.2 fmol L^{-1}. The MOF's porous framework also minimized interference in saliva samples, illustrating how MOFs enhance specificity by isolating targets from complex matrices.

6. Clustered regularly interspaced short palindromic repeat (CRISPR)-powered electrochemical genosensors

CRISPR-Cas systems have emerged as a breakthrough technology, offering attomolar detection limits, high specificity, and cost-effective workflows. CRISPR-Cas systems consist of guide RNA and Cas nucleases, classified into two classes based on effector complexity: Class 1 (multi-effector complexes) and Class 2 (single-effector proteins). CRISPR systems can be easily programmed using CRISPR-RNAs, identified and cleaved by either ssDNA or dsDNA. Recently, Cas-integrated electrochemical (E-CRISPR) sensors have been extensively employed to tackle the challenges of biomarker detection due to their highly selective affinity-based interactions with diverse biological targets. E-CRISPR bears all the working, counter, and reference electrodes, and Cas initiates cleavage of reporter strands only when complementarity is formed, resulting in the generation of electrochemical output signals. This versatile and straightforward CRISPR approach has been effectively incorporated into the development of sensors for various biologically significant analytes, including NA, protein and pathogen, and employed in genome engineering and transcription regulation. Huang et al. combined saltatory RCA (SRCA) and a CRISPR-Cas12a system to develop an electrochemical biosensor for the detection of *S. aureus*, one of the most common foodborne pathogens [62]. A GCE was modified with Au NPs, and a reporter probe with MB as an indicator signal was covalently immobilized. In the presence of *S. aureus*, tDNA was firstly amplified via SRCA and then recognized and combined with CRISPR RNA, activating the trans-cleavage activity of Cas12a and the cleavage of the reporter probe from the electrode surface. This biosensor exhibited superior sensitivity, compared to alternative electrochemical biosensors, and LOD values of 2.51 fg μL^{-1} for gDNA and 3 CFU mL^{-1} of *S. aureus* in pure cultures, respectively. This superiority was predominantly ascribed to the heightened amplification efficiency of SRCA and the distinctive trans-cleavage activity inherent in the CRISPR-Cas12a system. The incorporation of CRISPR enhanced the sensor's ultrahigh sensitivity and specificity for target detection. By CRISPR-Cas12a's specific recognition of the target, the likelihood of false-positive results arising from nonspecific amplification was diminished. In another study, He et al. developed a sensitive and rapid detection system to detect *Salmonella typhimurium* (*S. typhimurium*) by PCR and an E-CRISPR biosensor [63]. Specifically designed PCR primers ensured a perfect match with the tDNA sequence, endowing the E-CRISPR system with exquisite specificity to distinguish the bacteria of interest from non-tDNA. The E-CRISPR bacterial detection involved Cas12a-mediated cleavage and subsequent electrochemical detection. The electrochemical signal decreased dramatically when the second amplification of the extracted DNA of bacteria caused the release of electrochemical labels through activating the collateral cleavage activity of the Cas12a protein against signaling hairpin pDNAs. The design of hairpin DNA on the electrode increased the efficiency of Cas12a collateral cleavage by reducing the steric hindrance, which improved the detection performance of the electrochemical sensor in tDNA. Leveraging the high amplification capabilities of PCR on bacterial genes and the accurate tDNA recognition based on the CRISPR method, the E-CRISPR system attained a linear range from 6.7×10^1 to 6.7×10^5 CFU mL^{-1} with a LOD of 55 CFU mL^{-1} in pure culture, and 820 CFU mL^{-1} in spiked poultry meat. The detection of *S. typhimurium* in the poultry sample took <2.5 h.

Continuing the exploration of CRISPR-powered electrochemical genosensors, recent advancements have further demonstrated the versatility and precision of these systems in detecting a wide array of biological targets. These innovations leverage the unique properties of CRISPR-Cas systems, combined with novel signal amplification and transduction strategies, to achieve unprecedented levels of sensitivity and specificity. Li et al. introduced an electrochemical sensor that couples rolling circle amplification (RCA) with CRISPR-Cas12a to detect *E. coli*-2571 with exceptional sensitivity [64]. In their design, a double-stranded aptamer specifically binds to the target bacteria, which then competitively displaces a secondary aptamer. This displacement triggers T4 ligase-mediated circular DNA formation, and subsequent RCA produces long strands of ssDNA. These ssDNA fragments activate the trans-cleavage function of CRISPR-Cas12a, which in turn cleaves ferrocene-labeled probes on a gold electrode, altering the electrochemical signal. The sensor covers a linear detection range from 10^2 to 10^7 CFU mL^{-1} and reaches an LOD of 5.28 CFU mL^{-1}, a value that is surpassed the sensitivity of conventional chemiluminescence biosensors (LOD of 130 CFU mL^{-1}). Moreover, specificity assessments showed negligible cross-reactivity with *S. aureus, Salmonella*, and other *E. coli* strains, while tests on real-world samples (e.g., pure water and milk) resulted in recoveries between 93 and 101.5 %. By integrating RCA's powerful amplification with the precise cleavage of CRISPR-Cas12a, the approach minimizes background noise and offers a rapid, cost-effective, and highly specific method for pathogen detection, with potential applications in both clinical and environmental monitoring. Building on the theme of NA detection, Nguyen et al. developed an electrochemical biosensor that bypasses NA amplification by leveraging CRISPR-Cas9 for the simultaneous detection of HPV 16 and HPV 18 L1 genes [65]. A Cas9-sgRNA complex then precisely cleaves the target DNA, releasing fragments tagged with either MB or ferrocene, which generate distinct electrochemical signals. The sensor exhibits a wide dynamic range from 1 fmol L^{-1} up to 10 nmol L^{-1} and achieved remarkably low limits of detection (0.4 fmol L^{-1} for HPV 16 L1 and 0.51 fmol L^{-1} for HPV 18 L1), performance that rivaled RT-PCR. The inherent specificity of the CRISPR-Cas9 mechanism minimizes false positives through accurate target recognition. In a similar vein, Fan et al. reported an amplification-free electrochemical sensor that integrates antimonene nanosheets (Sb NSs) with CRISPR-Cas12a for NA detection [66]. In this method, a gold electrode was modified with Sb NSs to enhance the adsorption of ssDNA, which was then decorated with MB-labeled reporters. Upon recognition of the target DNA, the trans-cleavage activity of CRISPR-Cas12a non-specifically cut the labeled ssDNA, causing a drop in the electrochemical signal as detected by square wave voltammetry (SWV). The sensor could detect SARS-CoV-2 DNA down to 1.0×10^{-16} mol L^{-1} within 35 min, and it exhibited excellent specificity against non-target viruses (e.g., MERS, H1N1) and even single-base mismatches. The sensor demonstrated remarkable stability (to 8 weeks) and

reproducibility (over 50 cycles), while its integration with a portable SPCE made it highly suitable for point-of-care applications. The large surface area of Sb NSs, coupled with CRISPR's precision eliminated the need for further NA amplification. A biosensor that combined CRISPR-Cas13a with catalytic hairpin assembly (CHA) for the ultrasensitive detection of dengue virus (DENV) RNA was designed [67]. Their device employed a gold electrode modified with a reporter RNA-silenced DNA walker (DW) alongside a hairpin structure (H1). When DENV RNA was present, it activated the trans-cleavage activity of CRISPR-Cas13a, leading to release DW to initiate CHA. The released DW opens H1, thereby exposing a binding site for ferrocene-labeled hairpin 2, which significantly amplified the electrochemical signal. This biosensor offered a linear detection range from 5 fmol L^{-1} to 50 nmol L^{-1} and an LOD of 0.78 fmol L^{-1}, and it demonstrated high specificity by effectively discriminating against non-target DENV serotypes and random RNA sequences. Clinical testing using extracted RNA confirmed a robust correlation with standard methods. The amplification-free design, which marries the precision of CRISPR with the signal enhancement provided by CHA, enabled rapid (90 min) and portable diagnostics, with easy adaptability to other RNA targets via simple modifications of the crRNA sequence. In another study, Wu et al. advanced the field by developing an amplification-free E-CRISPR tailored for detection of the SARS-CoV-2 Delta variant [68]. Their approach integrated CRISPR-Cas12a with AuNP-modified electrodes, where AuNPs boost both electrical conductivity and probe immobilization. MB-labeled ssDNA serves as a reporter, when tDNA was present, the trans-cleavage activity of CRISPR-Cas12a cleaved the reporter, leading to a measurable decrease in the electrochemical signals. The sensor operated over a linear range from 100 fmol L^{-1} to 10 nmol L^{-1} and achieved an LOD of 50 fmol L^{-1}, while exhibiting high specificity by distinguishing non-target viruses (such as MERS and influenza) and differentiating the Delta variant from the wild-type strain. Clinical evaluations using both synthetic and extracted RNA samples yielded results that strongly correlated with fluorescence-based assays. Moreover, the biosensor's integration with a portable SPCE and a wireless micro-electrochemical platform enabled point-of-care testing within one hour, and its programmable crRNA allowed swift adaptation to emerging SARS-CoV-2 variants. These studies collectively highlighted the transformative potential of CRISPR-powered electrochemical genosensors in achieving ultrasensitive, specific, and rapid detection of pathogens and NAs. By leveraging the unique properties of CRISPR-Cas systems and innovative signal amplification strategies, these platforms offered versatile solutions for clinical diagnostics, environmental monitoring, and point-of-care testing. Although CRISPR-powered biosensors significantly enhance the specificity and sensitivity of NA detection, further improvements can be achieved by incorporating NA amplification techniques.

7. Electrochemical genosensing after NA amplification

Integration of NA amplification methods, such as PCR or isothermal amplification, with electrochemical genosensors offers significant advantages in the detection of trace amounts of tDNA. However, challenges exist, including the need for sophisticated equipment for PCR-based amplification, which can be cumbersome for POC applications. Isothermal amplification methods address this limitation but may exhibit reduced sensitivity, compared to PCR. Balancing the benefits of amplification with the practical constraints of the chosen method is crucial for optimizing the performance of electrochemical genosensors in diverse applications, ranging from medical diagnostics to environmental monitoring [69–72]. In a study, the possibility of adapting PCR primers to helicase-dependent amplification for the detection of *Salmonella* (a gram-negative enteric bacilli and a zoonotic food-borne pathogen) by isothermal amplification of its DNA sequence was reported [69]. Detecting *Salmonella* with high sensitivity is not achievable without PCR and HAD. Marchlewicz et al. developed an electrochemical DNA biosensor to detect single-stranded tox gene fragments of the toxigenic Corynebacterium diphtheriae strain [73]. This genosensor was employed to diagnose the early stages of diphtheria. Probes were used as the loop-and-stem "hairpin" DNA sequences and amplified tox gene fragments in an asymmetric PCR reaction were detected. The biosensor signal was based on conformational changes within the probe, and the distance between the electrode surface and a redox marker tethered to the probe. Ye et al. developed a quickly responding electrochemical biosensor for detecting *Salmonella* using an invA genosensor [74]. In this work, PPy-functionalized reduced Gr oxide, HRP-streptavidin bio-functionalized Au NP, and PCR were employed as a transducer, a nanotag to amplify the detection signal via hydrogen peroxide enzymatic reduction in the existence of hydroquinone, and an amplification method. Target invA concentrations between 1.0×10^{-16} and 1.0×10^{-10} mol L^{-1} were linearly quantified with a LOD of 4.7×10^{-17} mol L^{-1}, and *Salmonella* was detected during 2 h from 9.6 to 9.6×10^{4} CFU mL^{-1} with a LOD of 8.1 CFU mL^{-1}.

New amplification methods are needed to substitute PCR to eliminate the need for an advanced thermocycler and make routine testing for NA cost-effective. Sensitive and specific techniques based on amplifying tDNA at a constant temperature, like loop-mediated isothermal amplification (LAMP), are appropriate alternatives [70,75]. In a study, a novel integrated POC platform was presented to detect *M. tuberculosis* using LAMP [70]. In this biosensor, the LAMP products were mixed with the Hoechst-33258 redox agent to prevent degradation by the existing trace nucleases in the reaction. The biosensor could detect up to 1 pg of the total DNA or 40 M. *tuberculosis* genomes. Ben Aissa et al. reported a genosensor for the detection of *E. coli* using a padlock probe and a subsequent rolling RCA step [76]. The sensing process could be integrated with magnetic particles (MPs) providing several benefits including pre-concentration of *E. coli* DNA using a target-specific magnetic probe and then amplification of bacterial DNA on MPs by employing RCA. Two different electrochemical readout approaches, direct and indirect methods, for the RCA amplicons on MPs, were tested. In the first case, the magnetic RCA product was labeled with a digoxigenin marker and then incubated with an anti-DIG-HRP antibody as an electrochemical reporter. In the second one, the detection process was carried out directly with an HRP marker. Having discussed the integration of NA amplification with electrochemical genosensors, it is crucial to examine their real-world applications in pathogen detection. The following section delves into the detection of bacterial pathogens, highlighting various genosensor designs tailored for different bacterial species.

8. Electrochemical genosensor of bacteria

Legionella pneumophila (*L. pneumophila*) as a gram-negative and fastidious bacterium causes Pontiac fever and Legionaries' disease. Due to the severe growth of this pathogen, molecular diagnostics based on DNA can be very important, especially because traditional culture methods are time-consuming, often requiring over a week, and may miss viable but non-culturable cells. The ability of *L. pneumophila* to enter the viable but non-culturable state highlights the need for more sensitive and rapid detection methods, as traditional culture-based approaches may miss these forms of the pathogen and lead to inaccurate results. DNA-based techniques, such as biosensors, allow for early and accurate identification by targeting specific genes, enabling timely intervention during outbreaks. These methods also overcome the limitations of culture-based detection, which can suffer from contamination and reduced sensitivity. *L. pneumophila* is one of the threatening pathogens with many challenges for its rapid and specific detection, making DNA-based molecular diagnostics crucial for public health management. Mobed et al. developed a novel electrochemical genosensor for the detection of *L. pneumophila* bacteria based on electrodeposited Au NPs/cysteamine [77]. Toluidine blue (TB) was an electrochemical redox marker to monitor hybridization reactions. Bacchu et al. developed an

electrochemical DNA biosensor for the selective detection of *Salmonella enterica serovar typhi* for early diagnosis of typhoid [78]. Au NPs and poly (cysteine) were used as a substrate in which an amine-labeled *Salmonella enterica serovar typhi*-specific pDNA was immobilized on its surface, and anthraquinone-2-sulfonic acid was used as a marker (Fig. 3A). A response range of 10^{-6} to 10^{-22} mol L^{-1} and 1.8×10^{5} to 1.8 CFU mL^{-1} with LODs of 6.8×10^{-25} mol L^{-1} and 1 CFU mL^{-1} were obtained. Li et al. introduced a label-free cloth-based super-sandwich electrochemical aptasensor to detect *S. typhimurium* [79]. A DNA super-sandwich (DSS) was generated by a hybridization reaction between two ssDNAs, in which MB was inserted in its grooves to amplify the current signal and enhance the detection sensitivity. Several aptamers are bound to target bacteria and form a complex of target bacteria-aptamers. Target bacteria are immobilized on the surface of the electrode by attaching the aptamers to the pDNAs. Then, another tail of the aptamers is hybridized with DSS. When the concentration of the target bacteria was increased, a more complex target bacteria aptamer was formed, which caused more DSS to attach to them. One of the main advantages of the proposed biosensor is that it doesn't need DNA extraction and amplification. Therefore, the detection was performed in less time and at a lower cost. A genosensor for sensitive and selective detection of *Acinetobacter baumannii* gene sequence was presented [80]. In this approach, a pDNA was adsorbed on the surface of CS-modified disposable pencil graphite electrodes, and the guanine oxidation signal was measured to quantify the hybridization (Fig. 3B). A LOD of 1.86 nmol L^{-1} and a linear response range of 5 to 150 nmol L^{-1} were achieved.

A rapid sputum test for the detection of *M. tuberculosis* was developed by Sailimiyan Rizi et al. [81]. A *M. tuberculosis* H37Rv specific 22-bp oligonucleotide within the IS 6110 sequence of the bacterium genome was detected by exploiting a PPy/Mxene nanocomposite. The modification process involved drop-casting of Ti3C2Tx MXene, prepared through the delamination process of synthesized Ti_3AlC_2 MAX phase in HCl/LiF solution, and electrodeposition of pyrrole on the surface. The ability of the proposed biosensor was evaluated by measuring the peak current of MB as a redox indicator, showing a linear range of 100 fmol L^{-1} to 25 fmol L^{-1}, and a LOD of 11.2 fmol L^{-1}. Cheng et al. investigated a sensitive electrochemical biosensor to detect *Chlamydia Trachomatis* [82]. This biosensor was built on a foundation of a bovine serum albumin (BSA) carrier and target-responsive DNA hydrogels supported by duplex-specific nuclease. Target rRNA can initiate the DNA hydrogel response, causing duplex-specific nuclease to continuously cut target rRNA, subsequently releasing a huge amount of HRP-labeled streptavidin (SA-HRP) that was previously encapsulated in the hydrogel. The gold electrode exploited a porous BSA layer with normal interstices after polishing, cleaning, and modifying steps to capture the released SA-HRP. The thiol-modified and biotin-modified pDNAs were then fixed in these interstices and assembled to be distributed on the electrode surface, which consequently stabilized the capture of SA-HRP. The redox reaction of 3,3′,5,50′-tetramethylbenzidine and hydrogen peroxide was then accelerated by SA-HRP, generating a detectable current signal that was equivalent to the concentration of *Chlamydia Trachomatis* 16S rRNA between 10 fmol L^{-1} and 25 mol L^{-1} with 5.8 fmol L^{-1} as a LOD (Fig. 3C). Biosensors can be applicable in the production chain of juice to detect *Alicyclobacillus acidoterrestris*. This thermophilic and acidophilic

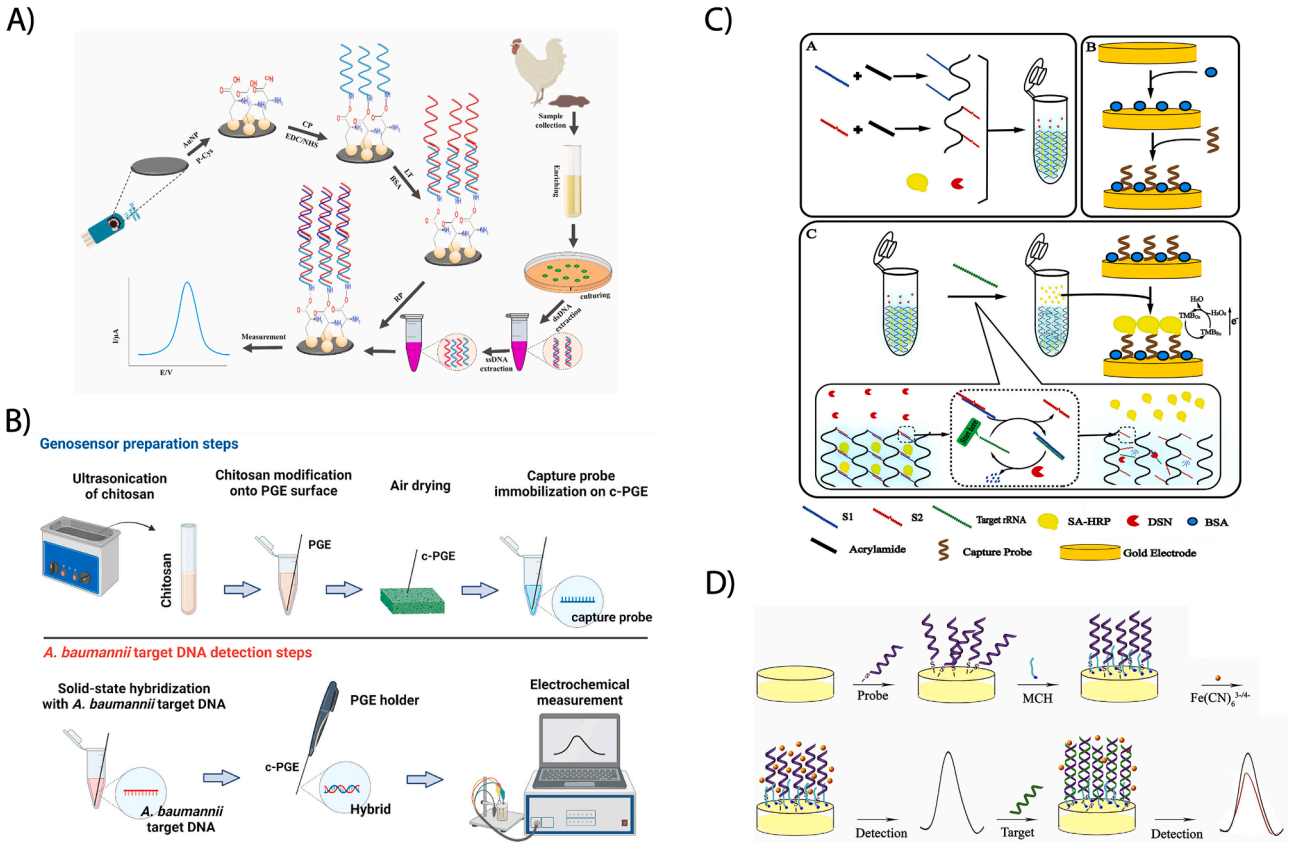

Fig. 3. A) Schematic presentation of fabrication of an electrochemical DNA biosensor using Au NPs and poly(cysteine) and detection of *Salmonella enterica serovar typhi*. Adapted with permission from [78]. Copyright 2022, Elsevier. B) A schematic view of assay protocol used for electrochemical sensing of *Acinetobacter baumannii* gene by a CS-modified disposable pencil graphite electrode. Adapted with permission from [80]. Copyright 2022, Elsevier. C) Schematic presentation of fabrication of an electrochemical biosensor to detect *Chlamydia Trachomatis*. A diagram for construction of target-responsive DNA hydrogels (A), a diagram for modification process of bovine serum albumin carrier platform (B), detection of *Chlamydia Trachomatis* based on DSN-assisted target-responsive DNA hydrogels and bovine serum albumin carrier platform (C). Adapted with permission from [82]. Copyright 2022, Elsevier. D) Fabrication and working steps of an electrochemical DNA biosensor for detection of *E. faecalis*. Adapted with permission from [87]. Copyright 2019, Elsevier.

bacterium is found in soil and is usually linked to the deterioration of acidic liquids and juices, such as orange juice. An electrochemical genosensor was introduced by Flauzino et al. to detect the genome DNA of *Alicyclobacillus acidoterrestris*, employing surface modification with poly (3-hydroxybenzoic acid) and reduced Gr oxide, and Hoechst 33258 (a common DNA stainer) as a marker [83]. Table 2 summarizes the key components and performance characteristics of various electrochemical genosensors developed for the detection of different bacterial pathogens.

E. coli is a pathogenic bacterium that plays a significant social and economic role in food safety and foodborne illness. Shi et al. developed a portable electrochemical biosensor for the detection of *E. coli* O157:H7 gDNA from chicken meat with controlling ability with a smartphone [84]. SPEs were first modified by in situ-produced and -functionalized nitrogen-doped carbonized polymer dots on a few black phosphorus film and then with Au NPs, and MB was a redox marker. tDNA was measured in a range of 1.0×10^{-19} and 1.0×10^{-6} mol L^{-1} with a LOD of 3.3×10^{-20} mol L^{-1}. *E. coli* was also measured using an electrochemical genosensor fabricated with animated hollow silica spheres-covered Au NPs, and anthraquinone was employed as a marker [85].

Detection of *Enterococcus faecalis* (*E. faecalis*), as a facultative anaerobic, gram-positive, and catalase-negative bacterium with the capability of surviving and growing under a variety of conditions, was studied by Nazari-Vanani et al. [86]. An ice crystal-like gold nanostructure was electrodeposited on a gold electrode surface as a transducer associated with a redox marker of TB. TB binding with both ssDNA and dsDNA was shortly studied showing the TB ability to discriminate between ssDNA and dsDNA. The LOD of this genosensor for the detection of EF gDNA was 30.1 ng μL^{-1}.

Further advancements include an electrochemical DNA biosensor for rapid and sensitive detection of *E. faecalis* [87]. This biosensor was constructed by immobilizing a specific pDNA, derived from the 16S rRNA sequence of *E. faecalis*, onto a gold electrode using SAMs. The biosensor exhibited a low detection limit of 3.3 amol L^{-1} for synthetic tDNA and could differentiate between single-, double-, and triple-missDNA with high selectivity (Fig. 3D). It quantified *E. faecalis* gDNA within the range of 1.1×10^{-7} to 1.1 ng mL^{-1}, with a detection limit of 7.1×10^{-9} ng mL^{-1}. The biosensor showed a relative standard deviation of 2.8 % without the need for pre-PCR amplification.

In the realm of *Brucella* detection, a highly sensitive electrochemical genosensor was developed using palladium NPs as a transducer [88]. This sensor was fabricated by electrodepositing palladium NPs onto a gold surface, facilitating the immobilization of a *Brucella*-specific pDNA. The genosensor demonstrated a detection limit of 2.7×10^{-20} mol L^{-1} and a linear concentration range from 1.0×10^{-12} to 1.0×10^{-19} mol L^{-1}. Performance validation included testing with cultured bacteria and human samples, with or without prior PCR amplification. The selectivity of the sensor against non-*Brucella* bacterial genomes was confirmed, underscoring its effectiveness for rapid *brucellosis* diagnosis.

Another development in *Brucella* detection involved an electrochemical genosensor featuring a 3D nanostructure of gold nanoribbons covered with gold nanoblooms [89]. This innovative design was achieved through sonoelectrodeposition on a gold surface, serving as a transducer for immobilizing a *Brucella*-specific pDNA. This architecture significantly increased the surface area and enhanced the immobilization of a *Brucella*-specific pDNA. The genosensor demonstrated a high sensitivity with a detection limit of 2.53×10^{-15} ng μL^{-1}, and a linear detection range from 1.07×10^{-14} to 1.07×10^{-2} ng μL^{-1}. It effectively differentiated between cDNA and mismatched DNA sequences and performed well with human serum samples without requiring PCR amplification. The combination of high sensitivity, rapid response, and cost-effectiveness of this sensor positions it as a significant advancement in molecular diagnostics, suitable for early bacterial infection detection in medical and environmental contexts. Beyond bacterial detection, electrochemical genosensors have also been successfully applied to detect parasitic infections. The next section explores advancements in genosensors for diagnosing parasites, focusing on their sensitivity, specificity, and real-world applicability.

9. Electrochemical genosensor of parasites

Trichomonas vaginalis (*T. vaginalis*) is one of the most commonly colonizing parasites, endangering public and human health by causing a Trichomoniasis infection. A label-free electrochemical genosensor was developed by Delshadi-Jahromi et al. to detect the *T. vaginalis* gDNA [90]. In this study, a facile procedure was used to electrodeposit anisotropic-shaped Au NPs as a transducer, which was combined with TB as a redox marker. The anisotropic shape of the gold nanostructure expectedly amplified the electrochemical signal to improve the sensitivity and specificity of the genosensor. More tDNA concentrations led to capturing by the immobilized pDNA leading to a decrease in the peak current caused by the reduction of the redox marker. The electrochemical response of the genosensor was finally correlated with tDNA concentrations ranging from 1.0×10^{-19} to 1.0×10^{-12} mol L^{-1} with a low LOD of 3.1×10^{-20} mol L^{-1}. A similar label-free electrochemical biosensor focused on detecting the MR TV 29 18S ribosomal RNA gene from *T. vaginalis* utilized non-spherical Au NPs as the transducer substrate, electrodeposited onto an Au surface [91]. This sensor, which used DPV with a ferro/ferricyanide redox indicator, achieved a wide detection range from 1.0×10^{-20} to 1.0×10^{-12} mol L^{-1}, and a LOD of 2.1×10^{-21} mol L^{-1} for synthetic DNA and 68.9 ng mL^{-1} for gDNA (Fig. 4A). It demonstrated high selectivity, distinguishing between cDNA, non-complementary DNA (ncDNA), and mismatched DNA sequences.

Another study introduced an ultrasensitive, label-free electrochemical DNA biosensor for *T. vaginalis* detection, employing a poly (ortho-aminophenol) film as a nanotransducer and redox-active indicator [92]. The biosensor utilized a thiolated pDNA specific to *T. vaginalis*, immobilized on the surface of poly(ortho-aminophenol) film (Fig. 4B). Detection was achieved by DPV, with the biosensor demonstrating a LOD of 3.9×10^{-21} mol L^{-1} for synthetic cDNA and 1.0 pg μL^{-1} for gDNA. It effectively differentiated between cDNA, ncDNA, and mismatched sequences, showcasing high selectivity and reproducibility. Additionally, the biosensor demonstrated excellent reproducibility, long-term stability, and reusability over multiple cycles of hybridization and dehybridization.

In contrast, for the detection of *Leishmania* parasites, a range of electrochemical genosensors have been developed. One such sensor used cadmium sulfide nanosheets as the transducer material for detecting *Leishmania infantum (L. infantum)*, the causative agent of visceral leishmaniasis [93]. This impedimetric genosensor operated without labels or PCR amplification and achieved a wide dynamic detection range from 1.0×10^{-14} to 1.0×10^{-6} mol L^{-1} for cDNA, with a LOD of 0.81 fmol L^{-1}. It also detected *L. infantum* gDNA in the range of 5–50 ng μL^{-1} with a detection limit of 1.2 ng μL^{-1}, demonstrating excellent selectivity, reproducibility, and stability (Fig. 4C).

Nazari-Vanani et al. investigated another genosensor for *L. infantum* using non-spherical Au NPs, which provided a high surface area for pDNA immobilization [94]. The sensor, which employed TB as a hybridization indicator, achieved a detection limit of 0.2 amol L^{-1} and effectively distinguished between tDNA and mismatched DNA sequences (Fig. 4D).

For *T. vaginalis* detection, a label-free electrochemical genosensor was developed using anisotropic-shaped Au NPs electrodeposited onto a gold electrode as the transducer [95]. A specific DNA sequence from the parasite's genome was immobilized on these NPs, with TB as the redox marker to detect hybridization. The sensor displayed a detection range of 1.0×10^{-19} to 1.0×10^{-12} mol L^{-1} and a LOD as low as 3.1×10^{-20} mol L^{-1}. It effectively differentiated between cDNA, mismatched, and ncDNA sequences and was tested on human samples, showing results comparable to the PCR-gel electrophoresis method. The genosensor was stable for over 26 days with a relative standard deviation of 3.9 %, highlighting its reproducibility for practical applications.

Table 2
Electrochemical genosensors for detection of bacteria.

Analyte	Electrode	pDNA sequence	Nanomaterial(s)	Detection technique	Detection range	LOD	Ref.
L. pneumophila	Au	5′-TCGATACTCTCCCCGCCCCTTTTGTATCGACG-3′	Au NPs	CV, SWV	1 μmol L^{-1}–1 zmol L^{-1}	1 zmol L^{-1}	[77]
Salmonella enterica serovar Typhi	SPCE	5′-TCTCTTAGCGCAAGCGACTG-3′	Au NPs and poly (ysteine)	DPV	For tDNA: 1×10^{-6}–1×10^{-22} mol L^{-1} For real *S. typhi. Typhi* samples: 1.8-1.8×10^{5} CFU mL^{-1}	For tDNA: 6.8×10^{-25} mol L^{-1} For real *S. Typhi* samples: 1 CFU mL^{-1}	[78]
S. typhimurium	SPCE	5′-TATGGCGGCGTCACCCGACGGGGACTTGACATTATGACAGTGTTACGGCGCTCTT-3′	N/A	DPV	10^{2}-10^{8} CFU mL^{-1}	16 CFU mL^{-1}	[79]
Acinetobacter baumannii	Pencil graphite	5'-TTITIAACTATTTACITCAICATIC-3'	CS	DPV	5-150 nmol L^{-1}	1.86 nM	[80]
M. tuberculosis	Glassy carbon	5′-CAAAGTGTGGCTAACCCTGAA-3′	Ti_3C_2 MXene nanosheets and PPy	DPV	100 fmol L^{-1}–25 nmol L^{-1}	11.24 fmol L^{-1}	[81]
Chlamydia trachomatis	Au	5'-TTTTTTTTTTTTTTTTTTTT-3'	N/A	Amperometry, EIS	10 fmol L^{-1}–25 pmol L^{-1}	5.8 fmol L^{-1}	[82]
E. coli	SPCE	5′-GGTCCGCTTGCTCTCGC-3′	N-CPDs, FLBP, Au NPs	DPV	1.0×10^{-19}–1.0×10^{-6} mol L^{-1}	3.33×10^{-20} mol L^{-1}	[84]
E. coli	SPCE	5′-GGTCCGCTTGCTCTCGC-3′	Aminated hollow silica spheres and Au NPs	DPV	1.0×10^{-12}–1.0×10^{-2} μmol L^{-1}	8.17×10^{-14} μmol L^{-1}	[85]
E. faecalis	Au	5′-CAATTGGAAAGAGGAGTGGCGGACG-3′	Ice crystals-like Au NPs	DPV	For synthetic tDNA: 1.0×10^{-17}–1.0×10^{-10} mol L^{-1} For genomic DNA: 100-160 ng μL^{-1}	For synthetic tDNA: 4.7×10^{-20} mol L^{-1} For gDNA: 30.1 ng μL^{-1}	[86]
E. faecalis	Au	5′-CAATTGGAAAGAGGAGTGGCGGACG-3′	N/A	DPV	1.1×10^{-7}–1.1 ng mL^{-1}	7.1×10^{-9} ng mL^{-1}	[87]
Brucella	Au	5′-TGCCGATCACTTAAGGGCCTTCAT-3′	Pd NPs	DPV	1.0×10^{-12} mol L^{-1}–1.0×10^{-19} mol L^{-1}	2.7×10^{-20} mol L^{-1}	[88]
Brucella	Au	5′-TGCCGATCACTTAAGGGCCTTCAT-3′	Au nanoribbons covered by Au nanoblooms	DPV	10 zmol L^{-1}–10 pmol L^{-1}	1.71 zmol L^{-1}	[89]

Additional abbreviations:
Nitrogen-doped carbonized polymer dots (N-CPDs).
Few-layer black phosphorus (FLBP).

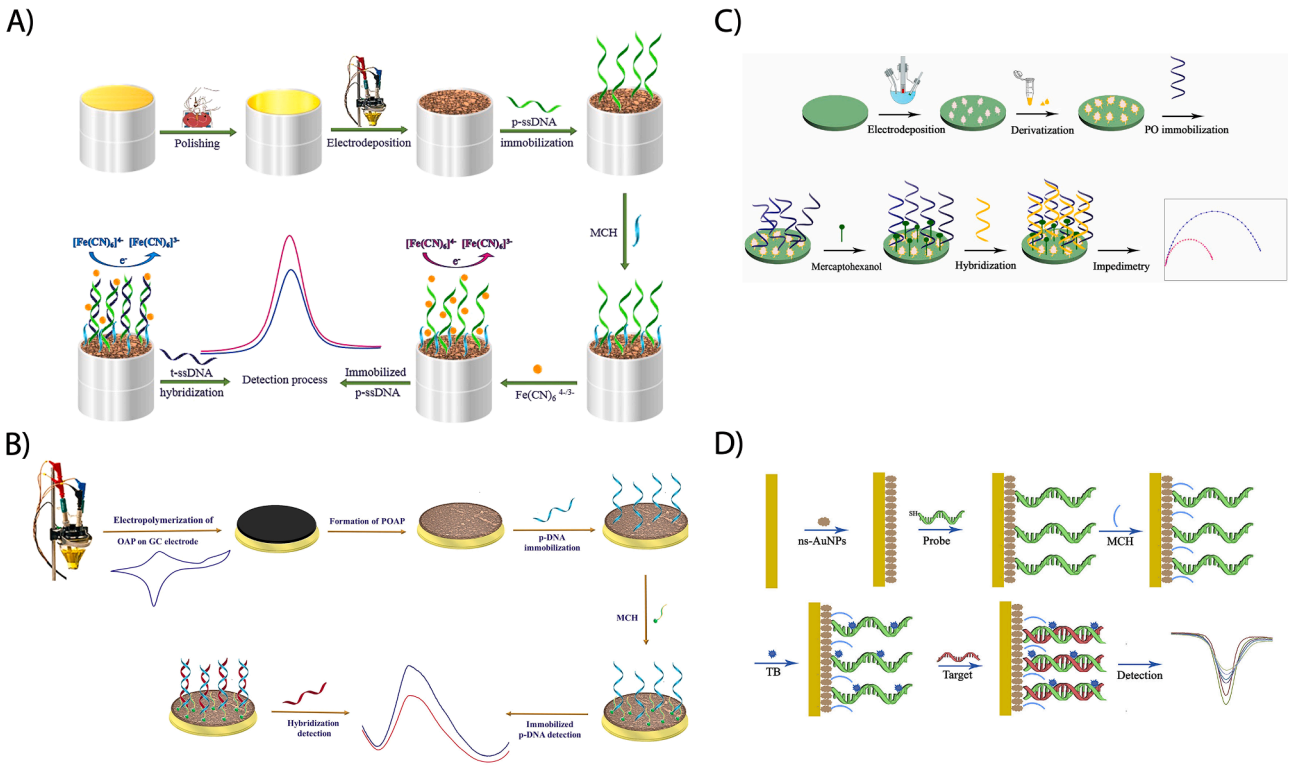

Fig. 4. A) Schematic presentation of fabrication and signal generation processes of a *T. vaginalis* biosensor. p-ssDNA, t-ssDNA and MCH denote pDNA, tDNA and 6-mercapto-1-hexanol, respectively. Adapted with permission from [91]. Copyright 2023, Elsevier. B) Fabrication steps of a *T. vaginalis* biosensor and c-DNA detection. OAP, MCH and p-DNA denote o-aminophenol, 6-mercapto-1-hexanol and pDNA, respectively. Adapted with permission from [92]. Copyright 2022, Elsevier. C) Fabrication procedures and signal generation mechanism of a *L. infantum* genosensor. PO denotes pDNA. Adapted with permission from [93]. Copyright 2020, Elsevier. D) Schematic presentation of an electrochemical genosensor for *L. infantum* kDNA genome using non-spherical Au NPs (ns-AuNPs). MCH denotes 6-mercapto-1-hexanol. Adapted with permission from [94]. Copyright 2018, Elsevier.

Further advancements for detecting *Leishmania major* (*L. major*) include the use of gold nanoleaves in an electrochemical biosensor [96]. The sensor operates without PCR amplification or labeling, employing a "signal-on" mechanism for enhanced sensitivity. Gold nanoleaves were electrodeposited onto a gold electrode with spermidine acting as a shape-directing agent during their electrodeposition. The unique structure of gold nanoleaves, resembling tree leaves, provides a high surface area that is advantageous for immobilizing pDNAs, thereby enhancing the biosensor's sensitivity and efficiency in detecting the tDNA. Spermidine was used to facilitate the formation of gold nanoleaves by influencing the morphology of the deposited gold. The presence of spermidine leads to the adsorption of an amine layer on the gold surface, which bears a positive charge due to the acidic conditions of the solution. This positive charge promotes further electrostatic adsorption of gold ions ($AuCl_4^-$), resulting in the nucleation and growth of gold nanoleaves on the electrode surface. This genosensor achieved a LOD of 1.8×10^{-20} mol L^{-1} for synthetic DNA and 0.07 ng μL^{-1} for gDNA, distinguishing *L. major* from other species with high selectivity. This approach is promising for diagnosing cutaneous leishmaniasis, especially in resource-limited settings.

Another label-free, PCR-free genosensor for *L. major* used gold hierarchical nanoleaflets synthesized with spermidine [97]. This sensor monitored DNA hybridization using ferrocyanide as a marker, detecting synthetic DNA with a detection limit of 2.98×10^{-21} mol L^{-1} and gDNA concentration of 0.11 ng μL^{-1}. The oxidation peak of ferrocyanide is recorded during DPV to assess the presence of hybridized DNA. The sensor was successfully applied to biopsy samples, offering a cost-effective and highly sensitive approach for clinical diagnostics without the need for PCR amplification.

Additionally, Heli et al. developed an electrochemical genosensor for *L. major* using cobalt-zinc ferrite quantum dots, providing a robust solution for parasitic DNA detection [98]. The quantum dots enhanced both pDNA immobilization and the electrocatalysis of MB, used as a redox marker. This genosensor detected synthetic DNA at concentrations as low as 2.0×10^{-19} mol L^{-1} and gDNA with a detection limit of 1.8×10^{-14} ng μL^{-1}. It exhibited high selectivity for *L. major* over other species such as *L. infantum* and *L. tropica*, detecting parasitic DNA from patient samples without the need for PCR amplification.

10. Electrochemical genosensor of fungi

Cryptococcal meningitis is a chronic disease with difficulty in early diagnosis and high morbidity and mortality. Liu et al. focused on easily detecting the DNA of *Cryptococcus neoformans* from cryptococcal meningitis patients [99]. They constructed an electrochemical DNA biosensor based on competitive assembly and homogeneous hybridization, not in the solid-liquid phase but in the solution phase, which resulted in higher hybridization efficiency and faster kinetics. For this purpose, two pDNAs captured the thermally denatured ssDNA. One pDNA was thiolated and immobilized on a gold electrode surface, and another biotin-labeled reporter pDNA was present in the solution phase. Thiolated pDNA was hybridized with one part of tDNA, and biotinylated pDNA was hybridized with another part of tDNA. Streptavidin-POD conjugate was also employed for enzyme-linked amperometric amplification. tDNA was successfully detected in a linear range between 5 pmol L^{-1} and 1 nmol L^{-1} with a LOD of 800 fmol L^{-1} (Fig. 5A).

A similar approach was used to develop an electrochemical genosensor for detecting *Candida auris* (*C. auris*), a multidrug-resistant fungal pathogen responsible for nosocomial outbreaks [100]. This genosensor leverages a gold electrode functionalized with a specific pDNA and employs ninhydrin as a novel hybridization indicator (Fig. 5B). Ninhydrin selective binding to dsDNA, as confirmed by theoretical

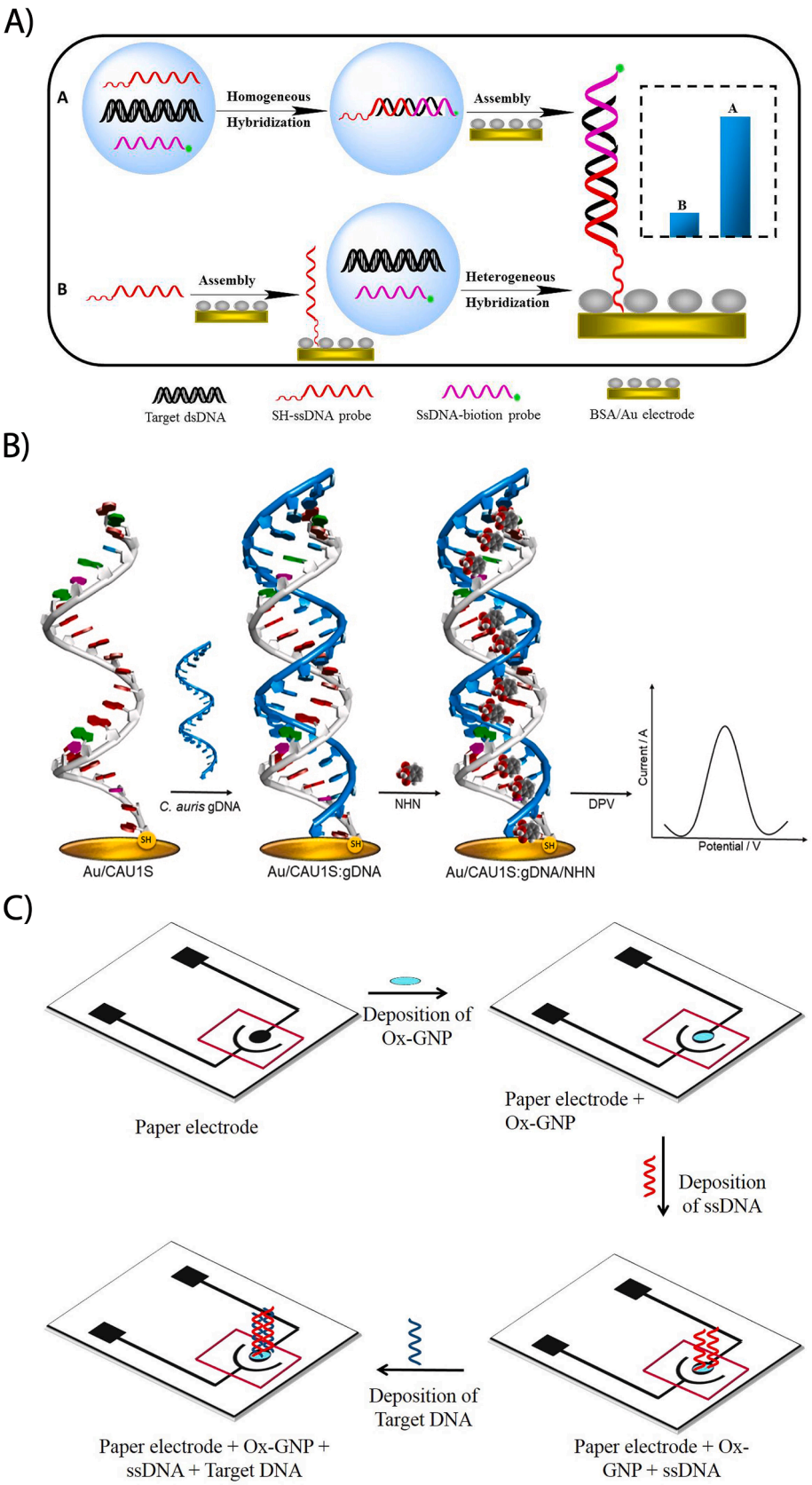

Fig. 5. A) Schematic illustration of electrochemical DNA sensors based on homogeneous and heterogeneous hybridization strategies, respectively. Adapted with permission from [99]. Copyright 2018, Elsevier. B) Schematic diagrams of the design of a reusable electrochemical genosensor for the detection of *C. auris* gDNA. Adapted with permission from [100]. Copyright 2021, Elsevier. C) Scheme of the graphene-based electrochemical DNA biosensor for the detection of *U. virens*. Adapted with permission from [101]. Ox-GNP denotes oxidised graphene nanoparticles.

calculations, provides a highly sensitive detection mechanism, differentiating it from conventional indicators. The sensor demonstrated a LOD of 4.5 pg μL^{-1} for *C. auris* gDNA in real samples like urine, with high selectivity, distinguishing *C. auris* from other pathogens such as *Candida albicans, E. coli*, and *Neisseria meningitidis*. It also maintained performance over eight hybridization cycles and exhibited 100 % signal stability after 80 days, making it a valuable tool for POC diagnostics due to its label-free, cost-effective, and simple design.

In agricultural pathogen detection, a Gr-based electrochemical DNA biosensor was developed for detecting *Ustilaginoidea virens*, the causative agent of false smut in rice [101]. This biosensor utilizes oxidized Gr NPs, enhancing conductivity and sensitivity. The device operates on a paper-based electrochemical platform, offering an eco-friendly and cost-effective alternative to traditional metal or glass electrodes. A pDNA specific to the fungal pathogen is used, with hybridization detected via cyclic and linear voltammetries and MB serving as the intercalating indicator (Fig. 5C). The biosensor showed a LOD of 10 fmol L^{-1} and exhibited excellent selectivity, distinguishing between cDNA and ncDNA sequences. The integration of oxidized Gr NPs improved the biomolecule interaction and enhanced the sensitivity and detection limit of the sensor, making it a promising tool for early and in-field detection of *Ustilaginoidea virens* in rice.

11. Electrochemical genosensor of viruses

For hepatitis B virus (HBV) detection, an electrochemical genosensor was developed based on poly(4-aminophenol) [42]. This genosensor utilizes a specific pDNA targeting the HBV DNA sequence and offers two detection methods: direct detection via the oxidation of guanine and adenine bases and indirect detection using ethidium bromide as a hybridization indicator. In the indirect method, ethidium bromide intercalates into the dsDNA formed during hybridization, increasing the oxidation current measured (Fig. 6). The sensor achieved a detection limit of 2.61 nmol L^{-1} and demonstrated high sensitivity and selectivity for cDNA sequences, while also distinguishing ncDNA and mismatched sequences. AFM confirmed the functionality of the sensor, offering visual evidence of hybridized and non-hybridized surfaces. The capability of this genosensor for real sample analysis and rapid detection makes it a promising tool for diagnosing HBV and other DNA-based viral diseases. Similarly, a polymer-based electrochemical genosensor was designed for the detection of Epstein-Barr Virus (EBV) [43]. This sensor utilized poly (4-aminothiophenol) and a specific pDNA for EBV. It also employed dual

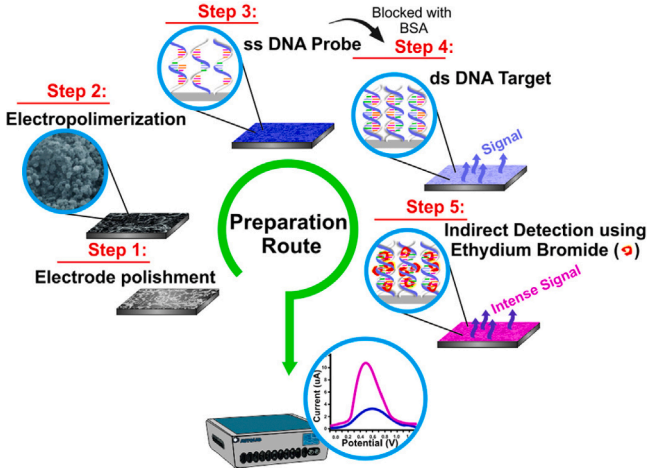

Fig. 6. Schematic presentation of preparation route for an electrochemical DNA biosensor, including electrode polishing, surface modification via electropolymerization, pDNA immobilization, blocking with BSA, tDNA hybridization, and indirect detection using ethidium bromide. Adapted with permission from [42]. Copyright 2014, Elsevier.

detection methods, with direct detection through DNA base oxidation and indirect detection, using ethidium bromide intercalation. The sensor demonstrated a detection limit of 17.32 nmol L^{-1} and effectively differentiated between cDNA, ncDNA, and single-missDNAs, ensuring high specificity for EBV. Furthermore, it maintained stability over 120 days and exhibited resistance to interference from common biological substances, highlighting its potential for clinical applications in detecting EBV-related diseases such as infectious mononucleosis and associated malignancies.

Yahyavi et al. introduced a NA-based electrochemical biosensor for the detection of influenza B virus using Au NPs [102]. In this study, a specific pDNA targeting the conserved nucleoprotein region of the B/Victoria/2/87 influenza virus was immobilized onto an Au NPs-modified electrode. The increased surface area provided by the Au NPs enhanced the sensor's sensitivity, enabling the detection of viral sequences. The biosensor exhibited high specificity and successfully distinguished cDNA, mismatched, and ncDNA sequences. Its performance was validated against real-time PCR in clinical samples, where it showed full agreement, confirming its reliability. With an operational stability of at least 25 days, this genosensor offers a rapid, sensitive, and cost-effective solution for detecting influenza B and other viral pathogens in clinical diagnostics.

Another approach involved the development of an electrochemical biosensor for detecting influenza A virus, utilizing meso/macroporous cobalt (II) oxide nanoflakes as the transducer material [103]. These nanoflakes, electrodeposited onto a platinum surface, provided a high surface area for the immobilization of a pDNA targeting the influenza A virus genome. This label-free genosensor detects DNA hybridization by measuring changes in current post-hybridization, without the need for pDNA modification or tagging, simplifying the fabrication process and reducing costs. The sensor demonstrated a detection limit of 86.4 amol L^{-1} for viral DNA and 0.28 ng μL^{-1} for RNA-derived cDNA. Its performance was validated in human samples, where significant changes in peak currents confirmed the presence of viral RNA in patient samples. The label-free design, combined with its high sensitivity and low-cost preparation, makes this biosensor a promising tool for viral detection in resource-limited settings, circumventing the limitations of traditional methods such as PCR. Table 3 provides a comprehensive summary of the electrochemical genosensors developed for the detection of parasites, fungi, and viruses, including their analytes, bioreceptors, nanomaterials, and detection ranges. While standalone electrochemical genosensors have demonstrated remarkable capabilities in pathogen detection, integrating them with microfluidic platforms further enhances their efficiency and portability.

12. A convergence of fields: electrochemical genosensors and microfluidics

Microfluidic electrochemical biosensing combines electrochemistry, biosensing, and microfluidics to enable portable, miniaturized diagnostic platforms [104–107]. Various types of microfluidic systems, such as lab-on-a-chip (LOC), paper-based, and digital microfluidics, are among the diverse array of platforms that have been developed [108, 109]. Each platform offers unique capabilities and can be tailored to specific analytical requirements. These systems enable precise manipulation of microliter-scale volumes, streamlining sample preparation, isolation, and detection in automated workflows. By harnessing the manipulation of fluid flow through microchannel networks, microfluidic systems offer a versatile approach to fabricating electrochemical sensors capable of detecting target analytes in complex matrices such as human blood.

12.1. Microfluidic modules for sample preparation

Before conducting the bioassay, various steps of sample preparation must be completed to examine the details of the sample. Identifying the

Table 3
Electrochemical genosensors for detection of parasites, fungi, and viruses.

Analyte	Electrode	pDNA sequence	Nanomaterial(s)	Detection technique	Detection range	LOD	Ref.
HBV	Graphite	5′-GAGGAGTTGGGGGAGCACATT-3′	poly(4-aminophenol)	DPV	1.89×10^{-9}-1.89×10^{-6} mol L^{-1}	2.61 nmol L^{-1}	[42]
EBV	Graphite	5′-AGGGATGCCTGGACACAAGA-3′	poly(4-aminothiophenol)	DPV	3.78-756 μmol L^{-1}	17.32 nmol L^{-1}	[43]
T. vaginalis	Au	5′-CATGTCCTCTCCAAGCGTAAGTACTGGGG-3′	Anisotropic-shaped Au NPs	DPV	1.0×10^{-19}–1.0×10^{-12} mol L^{-1}	3.1×10^{-20} mol L^{-1}	[90]
T. vaginalis	Au	5′-GAAGTCCTTCGGTTAAAGTTC-3′	Non-spherical Au NPs	DPV	1×10^{-20}–1×10^{-12} mol L^{-1}	2.1×10^{-21} mol L^{-1}	[91]
T. vaginalis	Glassy carbon	5′-GAAGTCCTTCGGTTAAAGTTC-3′	POAP	DPV	Synthetic tDNA: 1.0×10^{-20}–1.0×10^{-12} mol L^{-1} gDNA: 0.55-64 ng μL^{-1}	Synthetic tDNA: 3.9×10^{-21} mol L^{-1} gDNA: 1.0 pg μL^{-1}	[92]
L. infantum	Pt	5′-GTAATGTTACCCGATAGAAGTCTCGT-3′	CdS nanosheets	EIS	Synthetic tDNA: 1.0×10^{-14}–1.0×10^{-6} mol L^{-1} gDNA: 5-50 ng μL^{-1}	Synthetic tDNA: 0.81 f mol L^{-1} (6.5 fg mL^{-1}) gDNA: 1.2 ng μL^{-1}	[93]
L. infantum	Au	5′-ATCTCGTAAGCAGATCGCTGTGTCAC-3′	Non-spherical Au NPs	DPV	Synthetic tDNA: 1.0×10^{-18}–1.0×10^{-10} mol L^{-1} gDNA: 15-50 ng mL^{-1}	Synthetic tDNA: 2.0×10^{-19} mol L^{-1} gDNA: 9 ng mL^{-1}	[94]
T. vaginalis	Au	5′-CATGTCCTCTCCAAGCGTAAGTACTGGGG-3′	Anisotropic-shaped Au NPs	DPV	cDNA: 1.0×10^{-19}–1.0×10^{-12} mol L^{-1} gDNA: 50-85 ng μL^{-1}	cDNA: 3.1×10^{-20} mol L^{-1} gDNA: 48.1 ng μL^{-1}	[95]
L. major	Au	5′-AACCCACTAAAGCGTCACCCAACA-3′	Au nanoleaves	DPV	Synthetic tDNA: 1.0×10^{-19}–1.0×10^{-10} mol L^{-1} gDNA: 0.5-20 ng μL^{-1}	Synthetic tDNA: 1.8×10^{-20} mol L^{-1} gDNA: 0.07 ng μL^{-1}	[96]
L. major	Au	5′-AACCCACTAAAGCGTCACCCAACA-3′	Au hierarchical nanoleaflets	DPV	Synthetic tDNA: 1.0×10^{-12} to 1.0×10^{-20} mol L^{-1} gDNA: 0.5-15 ng μL^{-1}	Synthetic tDNA: 2.98×10^{-21} mol L^{-1} gDNA: 0.11 ng μL^{-1}	[97]
L. major	Carbon paste	5′-TGTTGGGTGACGCTTTAGTGGGTT-3′	Co-Zn ferrite quantum dots	DPV	Synthetic tDNA: 1.0×10^{-11}–1.0×10^{-18} mol L^{-1} For gDNA: 7.31×10^{-14}–7.31×10^{-6} ng μL^{-1}	Synthetic tDNA: 2.0×10^{-19} mol L^{-1} For gDNA: 1.80×10^{-14} ng μL^{-1}	[98]
Cryptococcus neoformans	Au	5′-GAGACGGGCAGAGTAACCCATACCGTCGAT-3′	N/A	Amperometry	5 pmol L^{-1}–1 nmol L^{-1}	800 fmol L^{-1}	[99]
C. auris	Au	5′-AACAAAACGAAAAAAAAAGCGTAGA-3′	N/A	DPV, EIS	4.5-45 ng μL^{-1}	4.5 pg μL^{-1}	[100]
Ustilaginoidea virens	Disposable paper-based	5′-TCTTGGCTCCTCGGAAGCTC-3′	Oxidized Gr NPs	CV, LSV	10 μmol L^{-1}–10 fmol L^{-1}	10 fM	[101]
Influenza B virus	Au	5′-GCCCGGAGTGAGACGAGAAATGCAG-3′	Au NPs	DPV	1.0×10^{-20}–1.0×10^{-10} mol L^{-1}	86.4 amol L^{-1}	[102]
Influenza A virus	Pt	5′-GGTTTTGGCCAGCACTACAGC-3′	*Meso*/macroporous CoO nanoflakes	DPV	Synthetic tDNA: 1.0 fmol L^{-1}–1.0 nmol L^{-1} cDNA: 0.5-10 ng μL^{-1} gDNA: 100-160 ng μL^{-1}	Synthetic tDNA: 86.4 amol L^{-1} cDNA: 0.28 ng μL^{-1} gDNA: 30.1 ng μL^{-1}	[103]

Additional abbreviations:
Cyclic voltammetry (CV).
Linear sweep voltammetry (LSV).

targets involves matching common pairs like antibodies/antigens, enzymes/substrates, DNA or RNA/their complementary sequences, and aptamers or bacteriophages/whole bacterial cells with diagnostic elements. Chip-scale extraction from biological samples has been achieved using various techniques that leverage miniaturization principles and physicochemical mechanisms. Most biological samples are a complex mixture of compounds, which can interfere with the analysis by masking the analyte of interest, reducing sensitivity or producing noise. Thus, a separation step is carried out before analyzing target molecules to eliminate unwanted materials that could lead to problematic interference. To investigate the desired molecules that are present inside a cell, it is necessary to first break down the cell to release the target molecules, and subsequently separate and isolate them. Integrated steps of cell lysis and NA extraction must be established to accomplish the precise, high-throughput NA analysis that will result in a comprehensive understanding of the biological system [110].

Typically, microfluidic devices for NA extraction follow a specific sequence of steps. Initially, the sample is introduced into the device through an inlet. Next, a lysis step occurs either within an inlet chamber or in a dedicated lysis module. The NAs are then captured in an extraction domain, where washing and elution phases occur, resulting in the extraction being withdrawn through an outlet port. Any waste generated during the process is usually collected in a designated area on the chip. In certain cases, such as RNA extraction, there may be a separate chamber for cDNA retrotranscription. While some of these procedures can be carried out either on the chip or off the chip, depending on the purpose and design of the device, others are fundamental to the NA extraction process and are typically performed on the chip itself [111].

12.1.1. *Cell lysis in a microfluidic system*

Different techniques have been devised for cell lysis on microfluidic platforms classified into four primary categories:

(i) Chemical lysis utilizes lysis buffers and detergents and is commonly employed to disrupt cell membranes and release cellular contents [112–114]. Chemical lysis can be categorized into alkaline and detergent lyses [112]. Alkaline lysis that uses hydroxide ions for cell disruption is suitable for various cell types but entails slow processing times of up to 12 h. Conversely, detergent lysis is more widely used for mammalian cells and necessitates additional steps for bacterial cells due to their protective outer cell wall [115]. Mild non-ionic detergents like zwitterionic detergent and Triton-X are preferred to minimize damage to proteins and enzymes [116]. Chemical lysis is favored in microfluidics for its simplicity [117].

(ii) Thermal lysis employs high temperatures to disrupt cell membranes, facilitating access to intracellular components by denaturing membrane proteins [118]. Temperature sensors are crucial for precise temperature control to prevent protein damage. Most thermal lysis methods utilize ohmic heating due to its low power consumption and scalability for microfluidic devices. Lee et al. developed an automated microfluidic device for DNA amplification, integrating micro heaters and temperature sensors to efficiently regulate temperature within the lysis chamber [119]. In another study, Packard et al. presented detergent-free, heat-only lysis on a microfluidic chip using *E. coli* cells, achieving efficient cell lysis and subsequent analysis of membrane compromise, protein, and DNA release. These advancements highlight the potential of thermal lysis in microfluidic applications [120].

(iii) Electrical lysis (also known as electroporation) is frequently employed for cell lysis, facilitating the creation of transient pores in the cell membranes by applying an external electric field. These pores release intracellular components once the transmembrane potential surpasses a specific threshold. Unlike chemical lysis with detergents, electroporation does not impact intracellular contents [121–123]. Devices for electroporation share similarities with mechanical and chemical methods in terms of flow-drive mechanisms. Typically, electrodes are made of materials like gold or platinum wire [124,125]. Various studies have reported the use of direct and alternating current (DC and AC) electric fields for lysis, addressing challenges such as gas bubble formation near the electrodes [124,126–129]. Researchers have designed innovative microfluidic chips with liquid electrodes, transparent ITO electrodes, and planar electrodes to achieve efficient, controlled, and rapid cell lysis under low-voltage conditions [130,131]. These advancements enhance the speed and effectiveness of cell lysis processes, demonstrating promising applications in various biological studies and analyses.

(iv) Mechanical lysis involves physically breaking down cell membranes using sheer force and direct damaging cell structures to release intracellular components [112]. A common approach integrates small nanoscale obstacles in microchannels to squeeze the cells and destroy their walls, ensuring sufficient shear stress. Capillary effects can also accelerate flow and increase shear forces in the lysis region [132]. Microfluidic systems, specifically lab-on-a-disk platforms, can be utilized to generate shear forces and disrupt cell membranes. Dehghan et al. employed a magnetic stirrer system with a rotating disk, where stationary magnets actuated a small stainless steel rotor, generating shear forces to effectively lyse the cells by disrupting their membranes during the rotation process [133]. Similar techniques involve using tiny and rotating ferromagnetic disks on a CD to swirl grinding beads and lyse cells, using an oscillating magnetic field [134]. Membranes can also be ruptured when cells are exposed to pressure waves with enough energy by using ultrasonic agitation [135]. Carlo et al. developed a device with sharp nanostructures to effectively penetrate cell membranes without harming extracted proteins [136]. Additionally, Han et al. utilized porous silica monoliths to mechanically lyse blood cells while allowing intact bacteria to traverse, enabling selective lysis based on the cell size and membrane tension [137]. This approach achieved high recovery rates of intact bacteria and effective sample preparation for downstream analysis. These advancements underscore the versatility and efficacy of mechanical lysis methods in microfluidic applications. Following cell lysis, the effective extraction and purification of NAs are paramount to ensure downstream detection accuracy. Microfluidic platforms have evolved diverse mechanisms for NA extraction, categorized by their underlying physicochemical principles.

12.1.2. *Microfluidic NA extraction*

Following cell lysis or NA release from the samples, numerous microfluidic sensing setups necessitate the purification or concentration of NA before its transfer to the sensor. Therefore, several methods for NA extraction have been devised within micro-total-analysis systems. These techniques can be classified based on the fundamental mechanisms underlying NA separation as field-assisted extraction, electrostatic interaction, membrane separation, and functionalized microparticles.

- Field-assisted extraction: The efficacy of sample preparation can be significantly enhanced by incorporating diverse energy fields, such as mechanical forces, and electrical, acoustic, and magnetic fields [138,139]. By chance, these forms of energy are frequently utilized in microfluidics to precisely manipulate substances and fluids at a minute scale. Consequently, most microfluidic setups are designed for analyte extraction, separation, or isolation relying on the aid of an external energy source. Based on the specific type of energy assistance, these techniques can be categorized into microflow-assisted extraction, centrifugal-assisted extraction, electric field-assisted extraction, acoustic-assisted extraction, and magnetic field-assisted extraction [140–146].
- Electrostatic interactions: Several NA extraction methods have been developed using electrostatic interactions between DNA and modified surfaces. These techniques typically utilize an amine-coated surface, where amine groups carry a positive charge at acidic pH levels, facilitating the binding of negatively charged DNA. However, the effectiveness of this method diminishes as the pH level becomes >7, posing challenges during the DNA amplification step due to the

high pH required for elution. To address this pH-related issue inherent in conventional electrostatic methods, researchers have explored the use of a CS-coated surface for DNA extraction from the whole blood. CS exhibits a cationic charge at pH=5 and can be readily neutralized at pH=9. Microfluidic channels featuring high-density CS coatings were developed and evaluated using lysed whole blood samples [110,147].

- Membrane separation: This technique integrates the membrane material into microchip devices, enabling miniaturized processes such as filtration, membrane extraction, and dialysis. NAs can adhere to silica or glass fibers in solutions with high ionic strength as electrostatic repulsion diminishes. Following washing with a non-polar solvent, DNA can be extracted using a low-ionic-strength buffer [110,147,148]. As an illustration, a silica membrane was enclosed within the middle of a multilayer assembly microchip platform and used to separate NAs from cellular debris post-bacterial lysis [149]. The refined NA of *E. coli* O157:H7 could be acquired in just 3 min, highlighting its viability for POC diagnostics. In handling biological specimens like cells, their physical and chemical attributes can be leveraged to implement membrane separation.
- Functionalized microspheres or magnetic beads: These beads with DNA adsorbent surfaces have also been deployed in various capacities for DNA extraction. MPs coated with functionalized carboxyl groups or silica have been employed to isolate DNA from biological specimens [110,150–154].

12.2. Integration platforms

Integrating multiple laboratory functions into microfluidic systems is highly desirable for on-site biosensing platforms. Compact microfluidic devices are well-suited for electrochemical sensors due to their reliability as molecular diagnostic platforms. Moreover, most measurement devices can directly interface with electrochemical signals, making the combination of microfluidics and electrochemical sensing a cost-effective and scalable approach for NA detection assays [155,156]. The integration of these technologies offers several advantages, including reduced sample and reagent consumption, shorter processing times, automated sample preparation and detection, high-throughput capabilities, multiplexed analysis within a single device, and improved portability and disposability [155,157–159].

Despite their high sensitivity and portability, electrochemical genosensors face several challenges in real-world applications, such as variability due to manual sample preparation, nonspecific binding in complex biological matrices, and technical difficulties in achieving multiplexed detection within miniaturized platforms. The integration of microfluidics effectively addresses these limitations by combining precise fluid control, automation, and system miniaturization, thereby enhancing sensor performance across multiple dimensions [160–162]. Specifically, microfluidic platforms augment electrochemical genosensors in the following ways:

- Minimizing nonspecific binding and background noise: Microfluidic channels enable controlled sample flow, reducing sample dispersion and surface fouling. This results in improved specificity and signal clarity, particularly in complex biological samples [163].
- Enhancing sensitivity and signal amplification: The ability to precisely manipulate fluid volumes within microchannels leads to increased analyte concentration, improving detection limits and signal-to-noise ratios. Additionally, efficient redox reactions facilitated by controlled microfluidic flow enhance electrochemical signal output [164].
- Enabling automated and high-throughput processing: Microfluidic integration allows for fully automated sample handling, minimizing human intervention and ensuring reproducibility. This is particularly beneficial for clinical diagnostics and point-of-care applications, where rapid and consistent results are essential [160].
- Facilitating multiplexed detection: Microfluidic architectures can accommodate multiple detection zones within a single device, enabling the simultaneous analysis of multiple targets. This is a crucial advancement for pathogen detection and disease diagnostics, where comprehensive screening is often required [160].
- Improving portability and field deployability: The miniaturized nature of microfluidic-electrochemical platforms reduces power and reagent requirements, making them ideal for point-of-care and field-based diagnostics. Unlike bulky optical biosensing systems, electrochemical microfluidic platforms offer robust and low-cost alternatives for rapid and decentralized testing [165].

By integrating these advancements, microfluidic electrochemical genosensors provide a more efficient, accurate, and scalable approach to NA-based diagnostics, bridging the gap between laboratory research and real-world applications.

Electrochemical microfluidic systems have proven advantages over conventional approaches in certain applications. For instance, Cheng et al.'s electrochemical microfluidic platform overcame the response constraints of the electrochemical biosensors that are used today [166]. Packed transducer materials between a top and bottom microelectrode characterize this microfluidic system. With the non-planar interdigitated electrode and the packed transducer material, a flow-through porous electrode was produced. Because of the special construction, each bound target or capture probe can be placed anywhere in the electrode or flow field and contribute to the overall signal, resulting in improved sensitivity and selectivity (Fig. 7A). This enables fmol L^{-1} sensitivity for DNA detection. Interestingly, a SAM-based stem-loop probe-modified gold microwire was used to create a woven-based microfluidic device [167]. Liquids were conveyed to the surface of the microwires/multifilament threads, which served as electrodes in the device, by utilizing the wicking property of the woven textile without the need for an extra pump. When combined with recombinase polymerase amplification, the fiber-based sensor could identify, in 65–70 min, gDNA from *Staphylococcus epidermidis* that was unpurified and isothermally amplified, with a detection limit of 10 copies/μL. These textile-based sensors could offer a substitute for POC NA diagnostics and wearable sensors (Fig. 7B).

Microfluidic platforms can also provide sample-to-answer solutions. Within a 3D-printed LOC platform, the automation of extracting, concentrating, and amplifying SARS-CoV-2 RNA from raw saliva was accomplished [168]. Specifically, to bypass the necessity of prior purification steps, processes involving viral lysis and nuclease inactivation were executed by adding a proteinase K solution at 55 °C, succeeded by an inactivation step at 95 °C. Moreover, a poly(ethersulfone) membrane was utilized to capture the NAs present in the saliva sample. Subsequently, the LAMP and CRISPR-based assays were carried out in distinct reaction chambers. This device facilitated the automated manipulation of liquids, starting from sample preparation up to the interpretation of signals. Moreover, this microfluidic chip incorporated a module for detecting host antibodies, thereby enabling the simultaneous analysis of multiple markers at the POC and supporting extensive monitoring of COVID-19 infections (Fig. 7C). In another study, a film-based microfluidic chip for POC was created by Park et al. to assess microorganisms causing foodborne diseases [169]. The chip combined solution mixing, electrochemical detection, and gene amplification functions. Its construction is made possible using patterned poly(ester) and poly(imide) sheets on a poly(carbonate) housing chip, which makes assembly and alignment straightforward. The platform allowed for the simultaneous amplification of the genes from foodborne pathogens using several microfluidic chambers and Hoechst 33258 for electrochemical detection. It may be manually constructed in 10 min. With the ability to identify *S. aureus* and *E. coli* at colony-forming unit concentrations as low as 10 and 100, respectively, this device exhibited high sensitivity and reproducibility. It can be used as a POC tool to screen different pathogens that cause foodborne illnesses (Fig. 7D).

Multiplexing detection is implied to be necessary to accurately

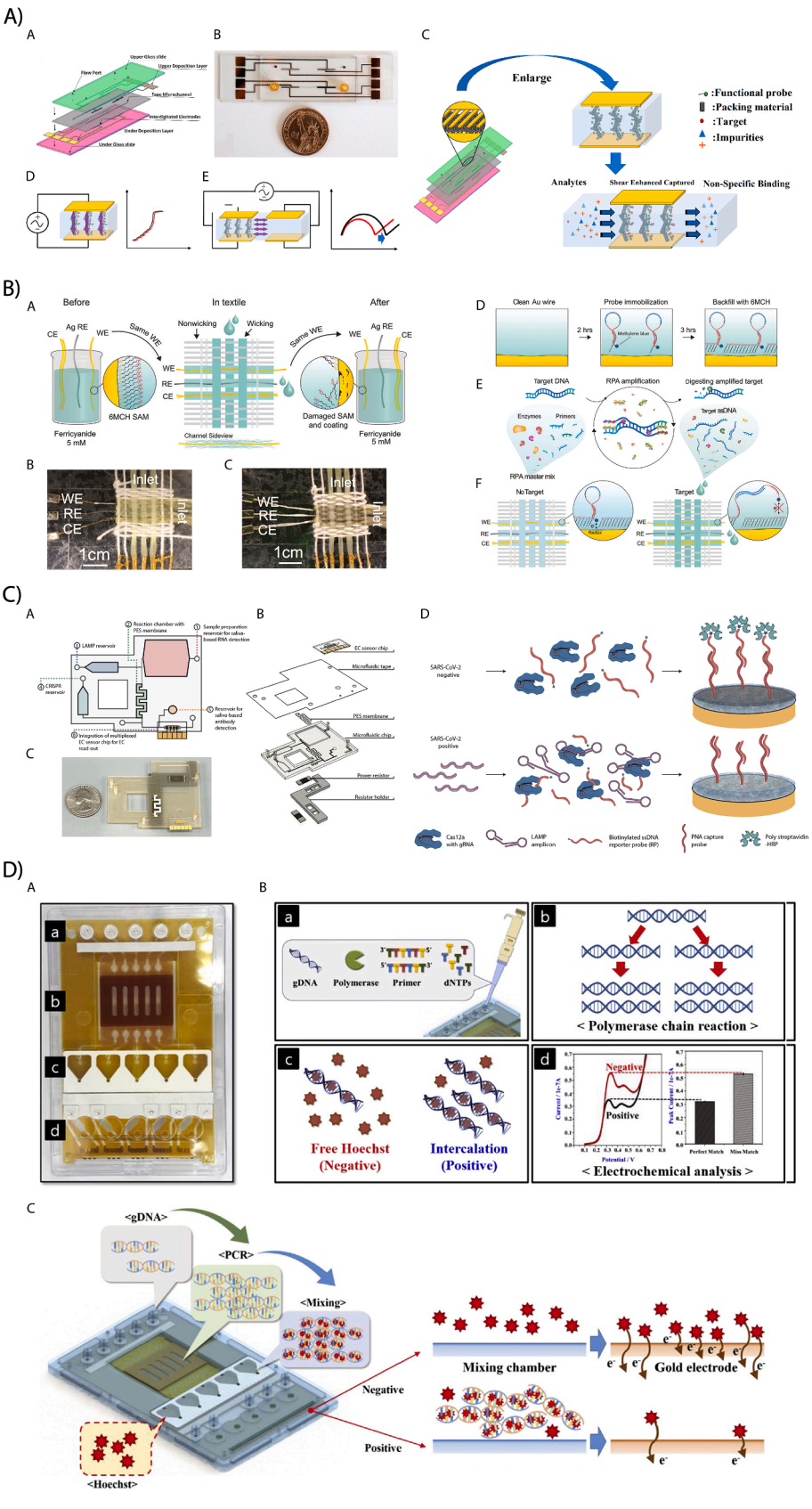

(caption on next page)

Fig. 7. A) An electrochemical sensor used a shear-enhanced, flow-through nanoporous capacitive electrode (ESSENCE). (A) Schematic diagram of assembled microfluidic device's different components. (B) A fully assembled ESSENCE chip. (C) Nano-ordered material with the functional capture probes packed in a microfluidic channel between two electrode arrays to form a porous structure. Due to the enhanced shear forces (from the packed electrode structure), the non-specific binding molecules will be washed away from the packing material's surface. (D) The material electrode (ME) behaving like a shorted electrode for conductive packing. (E) Using two ME electrode pairs together. The first pair was packed while the second pair was blank. The top and the bottom electrodes for each ME pair were shorted together. Adapted with permission from [166]. Copyright 2021, Elsevier. B) Microfluidic electrochemical biosensors for clinical diagnosis. Schematics of electrochemical DNA (E-DNA) sensor fabrication, integration into the Coolmax-weave, and isothermal amplification using recombinase polymerase amplification (RPA): (A) schematics of stepwise-electrochemical characterization of 6MCH-modified Au microwires and threads, MCH denotes 6-mercapto-1-hexanol; (B) and (C) photos of the real integrated microwires and Au multifilament threads into the woven microfluidic devices, respectively; (D) schematics of immobilization of MB conjugated stem-loop (S-L) DNA probes on the clean Au microwire surface and later backfilling of the electrode surface by 6MCH; (E) schematics of the mechanism of RPA and providing tDNA using lambda exonuclease enzyme for the detection step; (F) schematics of the woven E-DNA sensor into Coolmax-cotton weave. Copyright 2021, Wiley. Adapted with permission from [167]. Copyright 2021, Wiley. C) Schematic of CRISPR electrochemical assays and assay performance using clinical samples: (A) overview of the microfluidic chip designed for an LOC sample-to-answer saliva detection of SARS-CoV-2 RNA and antibodies; (B) an exploded view of the multiplexed system, which included a heater system, a sealed microfluidic chip and a multiplexed electrochemical sensor chip; (C) photograph of the microfluidic system with a quarter dollar for scale. (D) Schematic illustrating the surface chemistry of the EC assay. Without viral RNA (top row), the biotinylated ssDNA RP probe is not cleaved; therefore, the polystreptavidin-HRP binds to the PNA/ biotin-DNA duplex when added to the EC sensor chip and consequently precipitates TMB, resulting in an increase in current. In contrast, the biotinylated RP ssDNA is hydrolysed in the presence of viral target RNA (bottom row), cleaving the biotin group. Consequently, polystreptavidin-HRP does not bind to the surface of the chips, resulting in no TMB precipitation and no increase in current. Copyright 2022, Nature. Adapted with permission from [168]. Copyright 2022, Nature Portfolio. D) Scheme of a film-based integrated chip for pathogen analysis: (A) The fabricated integrated chip consisted of four parts: an inlet for solution injection, PCR chamber, mixing chamber, and detection area. The same configuration of five channels was designed for simultaneous detection of different pathogens on a single chip; (B) a schematic illustration of the functionalities and each part of the integrated chip; (C) The fluidic flow in the integrated chip. Adapted with permission from [169]. Copyright 2018, Elsevier.

diagnose some diseases. A few electrochemical microfluidic systems achieved this by creating subsections within their channel. For instance, the middle poly(dimethylsiloxane) layer of a 3D microfluidic platform had four sensing, four mixing, and four incubation zones that allowed for the simultaneous detection of four miRNAs [170]. MoS_2-$CuFe_2O_4$--based nanocomposites were synthesized to change the electrode due to their better catalytic activity and improved specific surface area to significantly boost the signal gain. This platform used for miRNA multiplexing detection based on 2D nanomaterials allows for POC diagnosis of paratuberculosis (Fig. 8A). Additionally, IMEAC, an integrated microfluidic electrochemical assay for cervical cancer, was introduced for the diagnosis of cervical cancer [171]. The device is noteworthy for utilizing a unique passive plasma separator that isolates plasma with no need to applying an external force. Since the separation is automated, hr-HPV16 cDNA can be found directly in an extracted plasma sample. When combined with an electrochemical sensor based on Gr oxide, a sample-to-answer workflow was accomplished with little manual intervention (Fig. 8B).

While microfluidic-electrochemical platforms enable simultaneous detection of multiple pathogens (e.g., S. aureus and *E. coli* in Park et al.'s work, Fig. 7D), several challenges hinder widespread adoption. First, cross-reactivity between probes remains a critical issue, as non-specific binding in complex biological matrices can generate false positives. For example, the IMEAC device (Fig. 8B) mitigates this by spatially separating plasma and antibody detection zones, but such designs increase device complexity and limit scalability. Second, signal interference arises when redox markers (e.g., methylene blue, ferrocene) with overlapping electrochemical signatures are used for distinct targets, complicating signal deconvolution. Third, probe design complexity escalates with the number of targets, requiring orthogonal immobilization strategies (e.g., MXene composites) to maintain hybridization efficiency. Material limitations, such as the finite surface area of electrodes for probe functionalization, further constrain multiplexing density. Addressing these challenges will require innovations in CRISPR-Cas systems for sequence-specific amplification, nanomaterials with tunable conductive properties, and AI-driven algorithms to resolve overlapping signals.

One type of microfluidic system that has gained popularity for POC clinical diagnostic applications is the paper-based analytical device. Paper-based materials have several advantages over other materials, including low cost, ease of manufacturing, high flexibility, disposability, and the ability to transport samples with no need for an externally driven force [172–174]. Miniaturization, mobility, low cost, and POC diagnosis are further characteristics of electrochemical biosensors that integrate with paper-based analytical tools. In this regard, Srisomwat et al. presented a paper-based electrochemical biosensor to detect HBV-associated [175]. They did this by utilizing an electrochemical lateral flow assay. This assay included both a gold metallization technique and a printed-delayed configuration. The sensing platform specifically has a straight non-delayed channel, a zigzag delayed channel, and a detecting zone. Gold pre-metallization was performed at the delayed channel zone, and pPNA was fixed on the detection zone with an electrode positioned underneath. DNA hybridization and gold metallization proceeded automatically and consecutively by utilizing this differential flow architecture (Fig. 9). The procedure took about 7 min to finish, demonstrating a potential molecular diagnostic platform without sacrificing sensitivity or selectivity.

Most microfluidic devices rely on the capture of the analyte using probes that have been fixed in specific regions of the microchannel of the device. In this instance, Ben-Yoav et al.'s work is relevant [155]. They created a dual-layer microfluidic valve array on poly(dimethylsiloxane) to create a microfluidic arrayed electrochemical LOC platform. 30-mer oligonucleotides were employed for label-free hybridization detection via EIS. Thiolated oligos were immobilized on a gold surface, and the flux was managed using a system of valved manipulation (Fig. 10A). They achieved a theoretical LOD of 1 nmol L^{-1}. This group used a diffusion-restriction model in a miniaturized biochip nanovolume reactor to precisely characterize DNA hybridization events in another investigation [176]. They concentrated on changes in diffusional resistance and charge transfer resistance. After the microfluidic biosensor was incubated with tDNA for 20 min, it showed selective detection of tDNAs with a calculated detection limit of 3.8 nmol L^{-1} and cross-reactivity of 13 %. The sensitivity of the biosensor was demonstrated by increasing impedance values at low frequencies to increase tDNA concentration. Charge transfer resistance and tDNA concentration had a semilogarithmic relationship (Fig. 10B). Kutluk et al. reported another interesting example [177]. They specifically focused on a disposable microfluidic technology for microRNA-197 (22-mer) electrochemical detection. The biotinylated pDNA was immobilized by first coating the microchannel with streptavidin and then obstructing it with biotin and BSA. An enzymatic reaction based on glucose oxidase was followed by an amperometric readout after the flux was stopped for a predetermined amount of time (stop-flow) (Fig. 10C). This biosensor, using 0.58 μL of the sample, yielded a LOD of 1.27 nmol L^{-1}.

Sfragano et al. presented an electrochemical assay conducted inside a tiny card-based device powered by microfluidic manipulation, requiring minimal amounts of consumables and human intervention [159]. The technique used DNA-modified MPs in conjunction with sample/signal

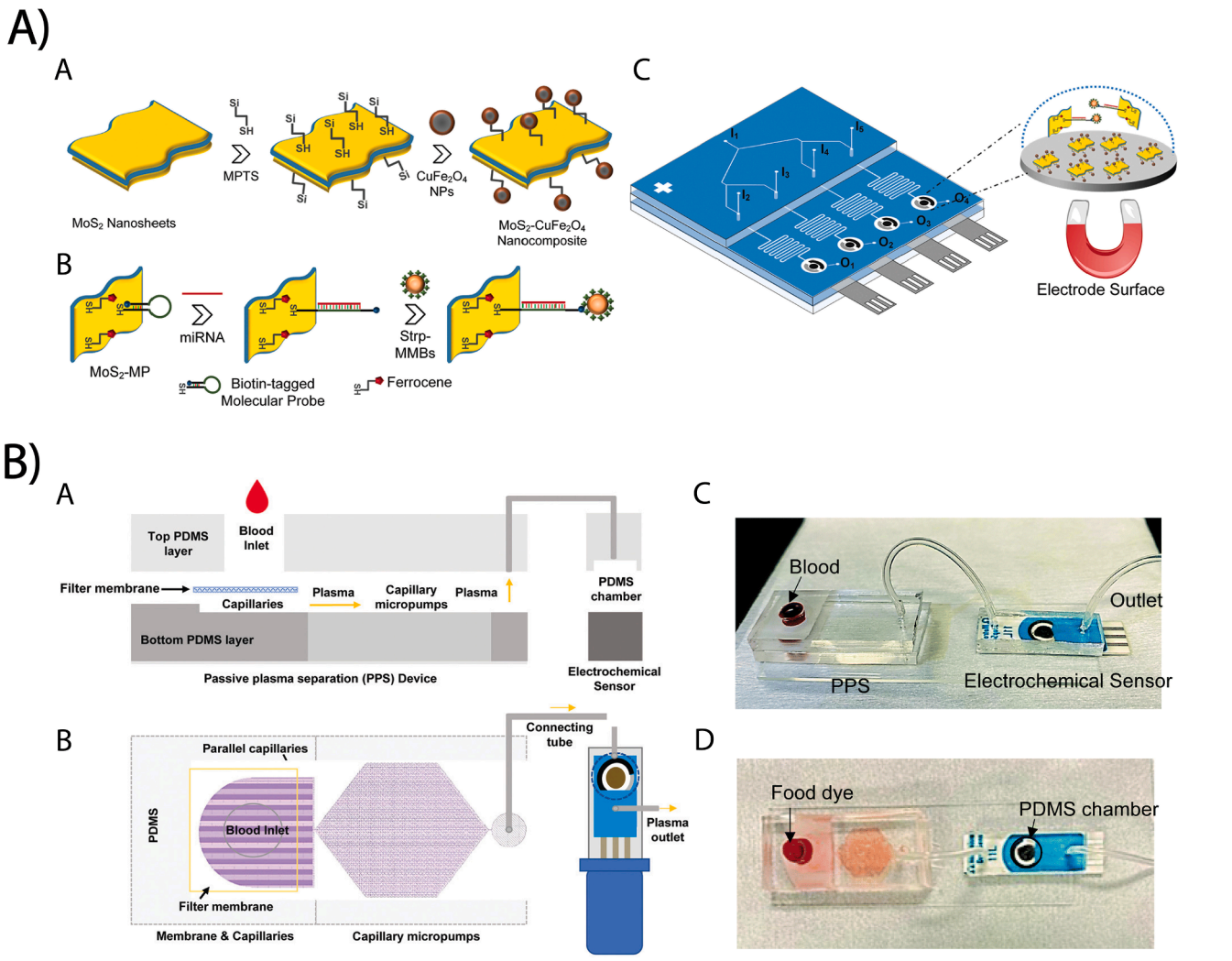

Fig. 8. A) MoS_2 nanosheets-based electrochemical miRNA sensor. (A) Schematic presentation of a MoS_2-$CuFe_2O_4$ nanocomposite synthesis, (B) principle of miRNA detection using MoS_2-MP nanocarriers, and (C) structure of the polydimethylsiloxane microfluidic platform showing inlets (I1–5), mixing zones, incubation zones, sensing zones, outlets (O1–4) and integrated electrodes, inset: miRNA detection on the nanocomposite modified electrode. MPTS denotes (3-mercaptopropyl) trimethoxysilane. Adapted with permission from [170]. Copyright 2018, Royal Society of Chemistry. B) Illustration of an integrated microfluidic electrochemical assay for cervical cancer detection: (A) and (B) side and top view of an integrated microfluidic electrochemical assay for cervical cancer (IMEAC) device that integrated two main modules: passive plasma separator (PPS) for plasma isolation and an electrochemical biosensor; (C) IMEAC was fabricated via connecting the outlet of the PPS device to the inlet of a chamber that covers the electrodes of the electrochemical biosensor using tubing; (D) a demonstration of the assay with food dye. Adapted with permission from [171]. Copyright 2022, Royal Society of Chemistry.

dual amplification to identify the results of DNA amplification. Identifying the sul1 and sul4 genes implicated in resistance to sulfonamide antibiotics is the main goal of the investigation. After being removed from *E. coli* cells, the resistance genes were amplified using an enzyme-assisted isothermal amplification technique. The low-cost and card-based setup that used microfluidic technology to examine the amplification products required little manual labor and small sample volumes. The platform successfully detected diluted amplification products of sul1 extracted from *E. coli* living cells in approximately one hour, with limits of detection of 44.2 pmol L^{-1} for sul1 and 48.5 pmol L^{-1} for sul4. This offers a potential method for identifying sulfonamide resistance genes in environmental and clinical matrices (Fig. 10D).

A technique for DNA trace analysis using on-chip pre-concentration, separation, and electrochemical detection in microchip gel electrophoresis using Au NPs to improve performance and sensitivity was presented [178]. Three parallel channels made up the microchip: one for microchip gel electrophoresis with electrochemical detection and two for field-amplified sample stacking and injection. Au NPs were added to the stacking and separation buffers to enhance pre-concentration and separation. The approach successfully examined a 100-bp DNA ladder including 13 fragments and demonstrated a considerable improvement in sensitivity.

The evolution of electrochemical microfluidic biosensors from foundational research to commercialization is clear. A wide range of materials-assisted electrochemical microfluidic systems have been used for a various goals, including low cost, wearability, and the elimination of the need for extra liquid manipulation. Multiplex detection, miniaturization, and sample-to-answer solutions are further research priorities for developing useful molecular diagnosis devices. Despite existing instances, the level of maturity remains restricted. The interdisciplinary character of the difficulties is becoming clearer; therefore, more advancements should be expected to suit broader scenarios. The following are the most crucial obstacles to be overcome: low sample volume and low Reynolds number, which affect sample preparation and fluid mixing; physical and chemical effects, such as capillary forces, surface roughness, and chemical interactions between analytes and construction materials; and low electrochemical signal-to-noise ratio, which is caused by the reduced surface area and volume [179]. These constraints result

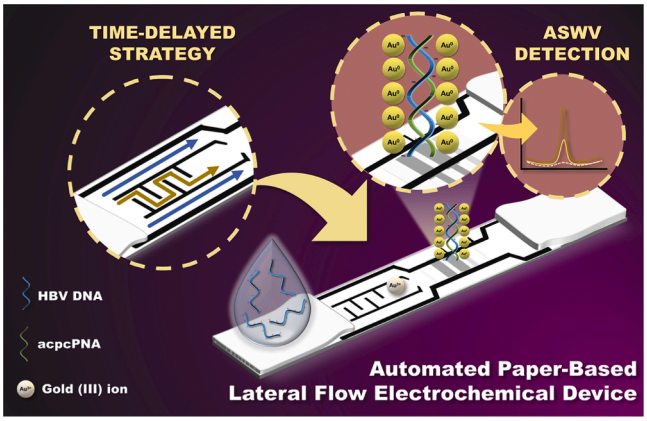

Fig. 9. Schematic illustration of the electrochemical lateral flow assay device for one-step HBV DNA detection. acpcPNA denotes pyrrolidinyl peptide nucleic acid. Adapted with permission from [175]. Copyright 2021, American Chemical Society.

in reduced density of probe surfaces, which alters their orientation; the presence of interfering oligonucleotides, which may induce mismatches; and limited mass transport and diffusion of tDNAs toward surface hybridization under static conditions [155]. By overcoming these obstacles, the development of miniaturized devices with several benefits for use in clinical settings could be accelerated. As research advances continue to push the boundaries of electrochemical genosensing and microfluidics, some of these innovations have transitioned from the laboratory to commercial applications. The final section discusses commercially available systems, their advantages, and remaining challenges in translating electrochemical genosensors into widespread clinical use.

13. Commercial systems

The concept of the microfluidic electrochemical biosensor has gained significant attention, leading to the commercialization of many versions of devices for portable POC analysis. An exemplary system that encompasses numerous features is the Abbott POC i-STATs System [180]. The analyzer is specifically designed to be used with a selection of cartridges that have enclosed microchannels. These microchannels are intended to process small amounts of whole blood depending on the specific type of cartridge. The cartridges allow for the measurement of 25 different substances and parameters related to blood chemistry. The detection method used is electrochemical, and many of the tests rely on catalytic biosensors (such as urea nitrogen, glucose, creatinine, lactate, ACT Celite, ACT Kaolin, and PT/INR), ion selective electrodes (such as Na^+, K^+, iCa^{2+}), or affinity biosensors (such as cTnI, creatine kinase-MB, and B-type natriuretic peptide). Although other microfluidic electrochemical POC devices have been fabricated, they still lack the necessary approval for diagnostic purposes. For example, an analogous portable gadget called the Nanomix eLab is used to identify cardiac biomarkers using cartridges [181]. Additional POC devices utilizing electrochemical biosensors are the Daktari CD4, an instrument designed for HIV diagnoses [182], and the Biosensia RapiPlex, which is used for

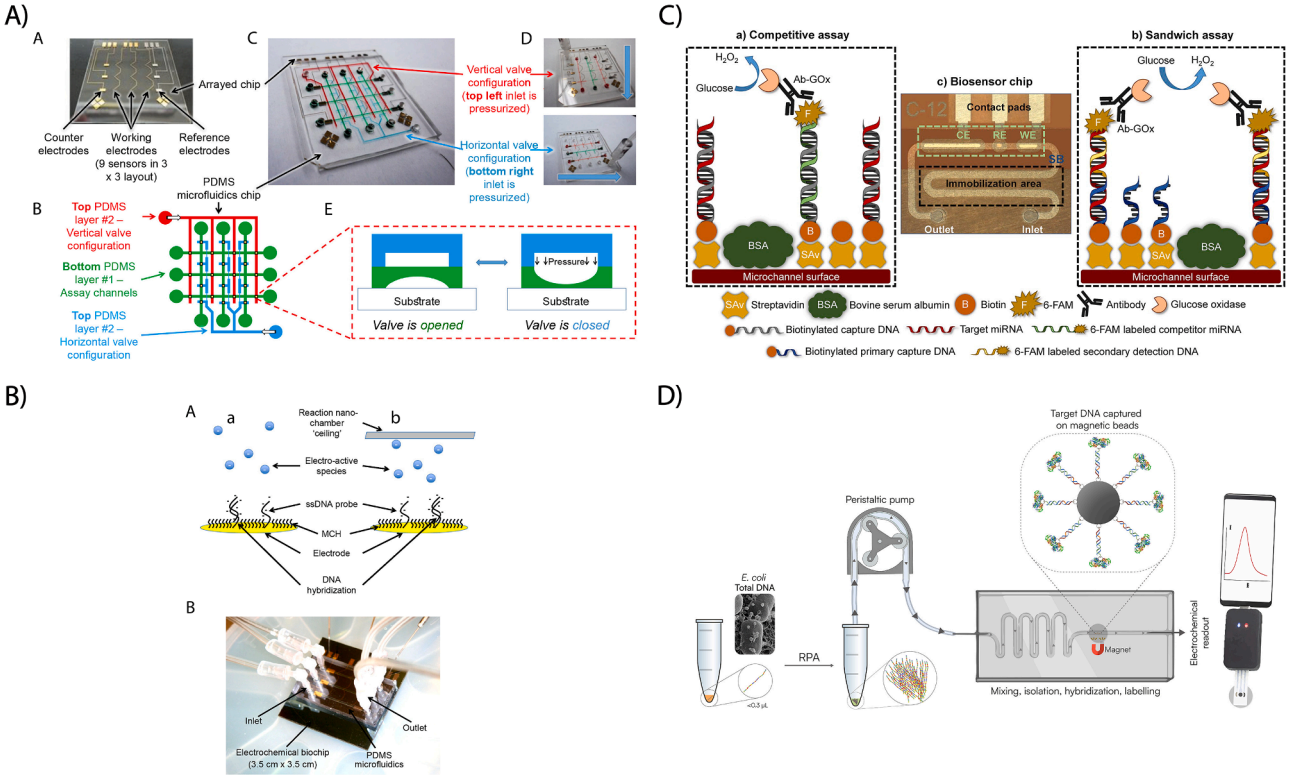

Fig. 10. A) Microfluidic-valved chip, showing (A) the fabricated arrayed electrochemical chip, (B) top valve configuration and the bottom assay channels, (C) entire assembled device, (D) vertical (top) and horizontal (bottom) valve configurations, and (E) valve actuation via the hydraulic channel to pinch off the microfluidic assay channel. Adapted with permission from [155]. Copyright 2015, Elsevier. B) The diffusion-based biosensing approach for (A) macro-scale biochips and (B) microfluidic-based biochips with the reflective boundary provided in the microfluidic biochips. Adapted with permission from [176]. Copyright 2012, Elsevier. C) Illustration of the (a) competitive and (b) sandwich assay formats that were employed for the detection of the target miRNA-197 on the microfluidic biosensor. (c) Image of the microfluidic biosensor, visualizing the immobilization area (black), the electrochemical cell with the counter, reference and working electrodes (green), and the stopping barrier (SB), shown in blue, which separates the two chambers. Adapted with permission from [177]. Copyright 2020, Elsevier. D) Schematic illustration of a microfluidic electrochemical detection system for analyzing sulfonamide resistance genes (e.g., sul1 and sul4) using DNA-modified magnetic beads [159].

electrochemical immunoassays for multiplexed detection [183].

14. Commercialization challenges and future directions

The development of biosensors is driven by the need to meet social demands through the creation of economically viable and effective biosensor devices. Despite their superior sensitivity and speed, electrochemical genosensors face commercialization challenges, including cost-effectiveness and scalability, which must be addressed to compete with optical biosensors. Notable technological instances of POC biosensors encompass LOC compact fluidic systems that have complete integration of sample preparation, PCR amplification, and electrochemical detection stages. Nevertheless, the expense of producing them may hinder their use in widespread applications by healthcare facilities, and other enhancements are required to eliminate the lengthy PCR amplification steps (2 h out of a total assay duration of 3.5 h). Nanopore DNA sequencing is now the most promising technology among existing options. It has a wide range of applications in scientific studies, and commercial tools are already being used for this purpose. Moreover, it remains uncertain if clinical nanopore diagnostic devices will achieve comparable levels of effectiveness.

Despite these advancements, several key challenges still hinder the scalability and deployment of genosensors for pathogen detection. Addressing these limitations is crucial for the effective translation of laboratory research into practical applications. One major challenge in the large-scale production of genosensors is maintaining batch-to-batch consistency while ensuring affordability. The fabrication of nanomaterial-based electrodes and microfluidic platforms often requires complex, high-cost manufacturing processes that hinder mass production. To address this, scalable printing techniques such as screen-printing or inkjet deposition of biomaterials have been explored [184, 185]. Additionally, integrating biosensors with disposable or reusable substrates can help lower costs while maintaining performance. For example, paper-based microfluidic devices have gained attention due to their low cost, ease of manufacturing, and disposability, making them ideal for resource-limited settings.

For field applications, genosensors must function reliably in diverse environmental conditions, from clinical settings to remote or resource-limited areas. Factors such as sample preparation complexity, stability of biological recognition elements, and the need for trained personnel limit practical deployment. Future efforts should focus on integrated, fully automated POC devices that minimize user intervention [186]. Moreover, regulatory approvals, including compliance with FDA and CE standards, remain a major hurdle for commercialization, requiring extensive validation studies.

The integration of microfluidics with electrochemical biosensors has shown immense potential in improving assay sensitivity, reducing sample volume requirements, and enhancing portability. Microfluidic platforms allow precise manipulation of fluids, enabling efficient sample pre-treatment, target enrichment, and multiplexed detection. Additionally, the use of microfluidic chips enables the automation of complex biochemical reactions, such as NA amplification and hybridization, within a miniaturized and cost-effective framework. Future research should focus on optimizing microfluidic flow dynamics to improve reaction efficiency, reducing clogging issues, and developing paper-based microfluidic sensors for resource-limited settings.

Detecting multiple pathogens simultaneously remains a significant bottleneck due to signal interference and cross-reactivity among different probes. Innovations in microarray-based electrochemical detection and barcode DNA technologies may enhance multiplexing capabilities [187]. Additionally, the development of AI-assisted signal processing algorithms could improve specificity and allow real-time analysis of complex biological samples.

Biofouling caused by the non-specific adsorption of proteins, cells, and other biomolecules can severely degrade sensor performance, leading to false positives or signal drift. To counteract this, researchers are exploring antifouling coatings, such as polyethylene glycol and zwitterionic polymers, as well as self-cleaning electrode surfaces [188]. Additionally, electrochemical pulse-cleaning strategies and enzymatic degradation approaches may offer promising solutions.

Future research should focus on integrating these strategies into genosensor platforms to create robust, scalable, and user-friendly diagnostic tools. The convergence of nanotechnology, automation, and AI-driven analytics is expected to drive the next wave of advancements, making genosensors a cornerstone of rapid and decentralized pathogen detection.

15. Conclusions and future outlooks

The convergence of electrochemistry, biosensors, and microfluidics is expanding the boundaries of conventional scientific and technical fields. This review comprehensively examines the various domains and their intersections, with a particular focus on applications. Although there are numerous types of microfluidic electrochemical biosensors designed for NAs, there appears to be a potential for developing novel techniques that can accurately measure tiny molecules like proteins and antibodies. Future advancements should prioritize multiplexed detection architectures using CRISPR-programmable systems and AI-assisted signal resolution to address co-infections and polymicrobial contamination. In addition to these prospects, microfluidic electrochemical biosensors encounter competition as other approaches become more affordable and compact. For instance, there are bench-top and personal mass spectrometers that can accomplish extremely specific detection without requiring biorecognition elements. However, despite this competition, progress in microfluidic electrochemical biosensors could potentially result in additional and even compatible technologies. Given the progress made thus far, we suggest that the intersecting fields of microfluidics, electrochemistry, and biosensors will continue to develop in unforeseeable ways. It is anticipated that this evolution will provide intriguing and perhaps significant ideas that could have a profound impact on our world.

CRediT authorship contribution statement

A. Dehghan: Writing – original draft, Investigation, Formal analysis, Data curation, Conceptualization. **M.J. Kiani:** Writing – original draft, Investigation, Formal analysis, Data curation, Conceptualization. **A. Gholizadeh:** Writing – original draft, Investigation, Formal analysis, Data curation, Conceptualization. **J. Aminizadeh:** Writing – original draft, Investigation, Formal analysis, Data curation, Conceptualization. **A. Rahi:** Writing – review & editing, Supervision, Project administration, Methodology, Conceptualization. **I. Zare:** Writing – original draft, Investigation, Formal analysis, Data curation, Conceptualization. **E. Pishbin:** Writing – review & editing, Project administration, Methodology, Conceptualization. **H. Heli:** Writing – review & editing, Validation, Supervision, Resources, Project administration, Funding acquisition, Conceptualization.

Declaration of competing interest

The authors declare that they have no known competing financial interests or personal relationships that could have appeared to influence the work reported in this paper.

Acknowledgments

We would like to thank the Research Councils of Shiraz University of Medical Sciences (31737) and Kerman University of Medical Sciences for supporting this research. The authors would also like to thank Center for Development of Clinical Research of Nemazee Hospital and, Dr. Nasrin Shokrpour for editorial assistance.

Data availability

Data will be made available on request.

References

[1] Geneva, Global Health Estimates 2016: Disease Burden by Cause, Age, Sex, by Country, and by Region, 2000-2016, World Heal. Organ., 2018.

[2] H.O. Kaya, A.E. Cetin, M. Azimzadeh, S.N. Topkaya, Pathogen detection with electrochemical biosensors: advantages, challenges and future perspectives, J. Electroanal. Chem. 882 (2021) 114989, https://doi.org/10.1016/j.jelechem.2021.114989.

[3] V. Rodovalho, L. Alves, A. Castro, J. Madurro, A. Brito-Madurro, A. Santos, Biosensors applied to diagnosis of infectious diseases - an update, Austin J. Biosens. Bioelectron. 1 (2015) 1–12.

[4] M. Datta, D. Desai, A. Kumar, Gene specific DNA sensors for diagnosis of pathogenic infections, Indian J. Microbiol. 57 (2017) 139–147, https://doi.org/10.1007/s12088-017-0650-8.

[5] T.S. Warfade, A.P. Dhoke, M.D. Kitukale, Biosensors in healthcare : overcoming challenges and pioneering innovations for disease management, (2025).

[6] U. Gupta, S. Yadav, K. Saini, M. Woollam, M. Agarwal, D. Maity, Chapter 4: a comparative study of the application of biosensors in Human health, Biosens. Technol. Hum. Health (2024) 70–107, https://doi.org/10.1039/9781837676323-00070.

[7] S. Menon, M.R. Mathew, S. Sam, K. Keerthi, K.G. Kumar, Recent advances and challenges in electrochemical biosensors for emerging and re-emerging infectious diseases, J. Electroanal. Chem. 878 (2020) 114596, https://doi.org/10.1016/j.jelechem.2020.114596.

[8] L.A. Wasiewska, F.G. Diaz, H. Shao, C.M. Burgess, G. Duffy, A. O'Riordan, Highly sensitive electrochemical sensor for the detection of Shiga toxin-producing *E. coli* (STEC) using interdigitated micro-electrodes selectively modified with a chitosan-gold nanocomposite, Electrochim. Acta 426 (2022) 140748, https://doi.org/10.1016/j.electActa2022.140748.

[9] K. Bialas, D. Moschou, F. Marken, P. Estrela, Electrochemical sensors based on metal nanoparticles with biocatalytic activity, Microchim. Acta 189 (2022) 172, https://doi.org/10.1007/s00604-022-05252-2.

[10] Y. Zhang, K. Zhang, H. Ma, Electrochemical DNA biosensor based on silver nanoparticles/poly(3-(3-pyridyl) acrylic acid)/carbon nanotubes modified electrode, Anal. Biochem. 387 (2009) 13–19, https://doi.org/10.1016/j.ab.2008.10.043.

[11] S.D. Bukkitgar, S. Kumar, S.Singh Pratibha, V. Singh, K.R. Reddy, V. Sadhu, G. B. Bagihalli, N.P. Shetti, C.V. Reddy, K. Ravindranadh, S. Naveen, Functional nanostructured metal oxides and its hybrid electrodes – recent advancements in electrochemical biosensing applications, Microchem. J. 159 (2020) 105522, https://doi.org/10.1016/j.microc.2020.105522.

[12] H. Beitollahi, S. Tajik, F.G. Nejad, M. Safaei, Recent advances in ZnO nanostructure-based electrochemical sensors and biosensors, J. Mater. Chem. B 8 (2020) 5826–5844.

[13] B.V. Salvi, P. Shende, Coordination bond- - based nanosystems for manipulating niche framework in biomedical applications, (2025). https://doi.org/10.1002/aoc.7978.

[14] D. Gao, Z. Ma, Y. Jiang, Recent advances in microfluidic devices for foodborne pathogens detection, TrAC Trends Anal. Chem. 157 (2022) 116788, https://doi.org/10.1016/j.trac.2022.116788.

[15] Y. Chen, Y. Liu, Y. Shi, J. Ping, J. Wu, H. Chen, Magnetic particles for integrated nucleic acid purification, amplification and detection without pipetting, TrAC Trends Anal. Chem. 127 (2020) 115912, https://doi.org/10.1016/j.trac.2020.115912.

[16] Y. Chen, N. Zong, F. Ye, Y. Mei, J. Qu, X. Jiang, Dual-CRISPR/Cas12a-assisted RT-RAA for ultrasensitive SARS-CoV-2 detection on automated centrifugal microfluidics, Anal. Chem. 94 (2022) 9603–9609, https://doi.org/10.1021/acs.analchem.2c00638.

[17] Y. Chen, Y. Mei, X. Jiang, Universal and high-fidelity DNA single nucleotide polymorphism detection based on a CRISPR/Cas12a biochip, Chem. Sci. 12 (2021) 4455–4462, https://doi.org/10.1039/d0sc05717g.

[18] N. Zong, Y. Gao, Y. Chen, X. Luo, X. Jiang, Automated centrifugal microfluidic chip integrating pretreatment and molecular diagnosis for hepatitis B virus genotyping from whole blood, Anal. Chem. 94 (2022) 5196–5203, https://doi.org/10.1021/acs.analchem.2c00337.

[19] Y. Chen, Y. Mei, X. Zhao, X. Jiang, Reagents-loaded, automated assay that integrates recombinase-aided amplification and Cas12a nucleic acid detection for a point-of-care test, Anal. Chem. 92 (2020) 14846–14852, https://doi.org/10.1021/acs.analchem.0c03883.

[20] R.L. Nouwairi, L.L. Cunha, R. Turiello, O. Scott, J. Hickey, S. Thomson, S. Knowles, J.D. Chapman, J.P. Landers, Ultra-rapid real-time microfluidic RT-PCR instrument for nucleic acid analysis, Lab Chip 22 (2022) 3424–3435, https://doi.org/10.1039/d2lc00495j.

[21] C. Wei, C. Yu, S. Li, J. Meng, T. Li, J. Cheng, J. Li, A droplet-based multivolume microfluidic device for digital polymerase chain reaction, Sens. Actuat. B 371 (2022) 132473, https://doi.org/10.1016/j.snb.2022.132473.

[22] Y. Zai, C. Min, Z. Wang, Y. Ding, H. Zhao, E. Su, N. He, A sample-to-answer, quantitative real-time PCR system with low-cost, gravity-driven microfluidic cartridge for rapid detection of SARS-CoV-2, influenza A/B, and human papillomavirus 16/18, Lab Chip 22 (2022) 3436–3452, https://doi.org/10.1039/d2lc00434h.

[23] Z. Li, X. Xu, D. Wang, X. Jiang, Recent advancements in nucleic acid detection with microfluidic chip for molecular diagnostics, TrAC Trends Anal. Chem. 158 (2023) 116871, https://doi.org/10.1016/j.trac.2022.116871.

[24] A. Parihar, S. Yadav, M.A. Sadique, P. Ranjan, N. Kumar, A. Singhal, V. Khare, R. Khan, S. Natarajan, A.K. Srivastava, Internet-of-medical-things integrated point-of-care biosensing devices for infectious diseases: toward better preparedness for futuristic pandemics, Bioeng. Transl. Med. 8 (2023) e10481, https://doi.org/10.1002/btm2.10481. PMID: 37206204.

[25] G.M. Whitesides, The origins and the future of microfluidics, Nature 442 (2006) 368–373, https://doi.org/10.1038/nature05058.

[26] J. Lum, R. Wang, B. Hargis, S. Tung, W. Bottje, H. Lu, Y. Li, An impedance aptasensor with microfluidic chips for specific detection of H5N1 avian influenza virus, Sensors 15 (2015) 18565–18578, https://doi.org/10.3390/s150818565.

[27] A. Sassolas, B.D. Leca-Bouvier, L.J. Blum, DNA biosensors and microarrays, Chem. Rev. 108 (2008) 109–139, https://doi.org/10.1021/cr0684467.

[28] H. Moustakim, H. Mohammadi, A. Amine, Electrochemical DNA biosensor based on immobilization of a non-modified ssDNA using phosphoramidate-bonding strategy and pencil graphite electrode modified with AuNPs/CB and self-assembled cysteamine monolayer, Sensors 22 (2022) 9420, https://doi.org/10.3390/s22239420.

[29] A. Mantz, A. Rosenthal, E. Farris, T. Kozisek, E. Bittrich, S. Nazari, E. Schubert, M. Schubert, M. Stamm, P. Uhlmann, A.K. Pannier, Free polyethylenimine enhances substrate-mediated gene delivery on titanium substrates modified with RGD-functionalized poly(acrylic acid) brushes, Front. Chem. 7 (2019) 51, https://doi.org/10.3389/fchem.2019.00051.

[30] C. Wittmann, DNA immobilization, in: R.A. Meyers (Ed.), Encyclopedia of Analytical Chemistry, Wiley, 2022, pp. 1–38, https://doi.org/10.1002/9780470027318.a9210.pub2.

[31] R. Campos, A. Kotlyar, E.E. Ferapontova, DNA-mediated electron transfer in DNA duplexes tethered to gold electrodes via phosphorothioated dA tags, Langmuir 30 (2014) 11853–11857, https://doi.org/10.1021/la502766g.

[32] X. Meng, D. O'Hare, S. Ladame, Surface immobilization strategies for the development of electrochemical nucleic acid sensors, Biosens. Bioelectron. 237 (2023) 115440, https://doi.org/10.1016/j.bios.2023.115440.

[33] J. Qiu, J. Tang, J. Shen, C. Wu, M. Qian, Z. He, J. Chen, S. Shuang, Preparation of a silver electrode with a three-dimensional surface and its performance in the electrochemical reduction of carbon dioxide, Electrochim. Acta 203 (2016) 99–108.

[34] L. Zhang, Z. Li, X. Zhou, G. Yang, J. Yang, H. Wang, M. Wang, C. Liang, Y. Wen, Y. Lu, Hybridization performance of DNA/mercaptohexanol mixed monolayers on electrodeposited nanoAu and rough Au surfaces, J. Electroanal. Chem. 757 (2015) 203–209.

[35] S. Campuzano, F. Kuralay, J. Wang, Ternary monolayer interfaces for ultrasensitive and direct bioelectronic detection of nucleic acids in complex matrices, Electroanalysis 24 (2012) 483–493.

[36] J. Wu, S. Campuzano, C. Halford, D.A. Haake, J. Wang, Ternary surface monolayers for ultrasensitive (zeptomole) amperometric detection of nucleic acid hybridization without signal amplification, Anal. Chem. 82 (2010) 8830–8837, https://doi.org/10.1021/ac101474k.

[37] M.A. Booth, K. Kannappan, A. Hosseini, A. Partridge, In-depth electrochemical investigation of surface attachment chemistry via carbodiimide coupling, Langmuir 31 (2015) 8033–8041, https://doi.org/10.1021/acs.langmuir.5b01863.

[38] B. Lakard, Electrochemical biosensors based on conducting polymers : a review, Appl. Sci. 10 (2020) 6614, https://doi.org/10.3390/app10186614.

[39] G. Wang, A. Morrin, M. Li, N. Liu, X. Luo, Nanomaterial-doped conducting polymers for electrochemical sensors and biosensors, J. Mater. Chem. B 6 (2018) 4173–4190, https://doi.org/10.1039/c8tb00817e.

[40] C. Liu, D. Jiang, G. Xiang, L. Liu, F. Liu, X. Pu, An electrochemical DNA biosensor for the detection of Mycobacterium tuberculosis, based on signal amplification of graphene and a gold nanoparticle-polyaniline nanocomposite, Analyst 139 (2014) 5460–5465, https://doi.org/10.1039/c4an00976b.

[41] D. Voccia, M. Sosnowska, F. Bettazzi, G. Roscigno, E. Fratini, V. De Franciscis, G. Condorelli, R. Chitta, F. D'Souza, W. Kutner, I. Palchetti, Direct determination of small RNAs using a biotinylated polythiophene impedimetric genosensor, Biosens. Bioelectron. 87 (2017) 1012–1019, https://doi.org/10.1016/j.bios.2016.09.058.

[42] A.C.H. Castro, E.G. Franca, L.F. de Paula, M.M.C.N. Soares, L.R. Goulart, J. M. Madurro, A.G. Brito-Madurro, Preparation of genosensor for detection of specific DNA sequence of the hepatitis B virus, Appl. Surf. Sci. 314 (2014) 273–279, https://doi.org/10.1016/j.apsusc.2014.06.084.

[43] R.P.A. Balvedi, A.C.H. Castro, J.M. Madurro, A.G. Brito-Madurro, Detection of a specific biomarker for epstein-barr virus using a polymer-based genosensor, Int. J. Mol. Sci. 15 (2014) 9051–9066.

[44] S. Mohan, P. Nigam, S. Kundu, R. Prakash, A label-free genosensor for BRCA1 related sequence based on impedance spectroscopy, Analyst 135 (2010) 2887–2893, https://doi.org/10.1039/c0an00258e.

[45] H. Peng, L. Zhang, J. Spires, C. Soeller, J. Travas-Sejdic, Synthesis of a functionalized polythiophene as an active substrate for a label-free electrochemical genosensor, Polymer 48 (2007) 3413–3419.

[46] N. Shoaie, M. Forouzandeh, K. Omidfar, Voltammetric determination of the *Escherichia coli* DNA using a screen-printed carbon electrode modified with polyaniline and gold nanoparticles, Microchim. Acta 185 (2018) 217, https://doi.org/10.1007/s00604-018-2749-y.

[47] N.T. Nguyet, V.V. Thu, H. Lan, T. Trung, A.T. Le, V.H. Pham, Simple label-free DNA sensor based on CeO2 nanorods decorated with ppy nanoparticles, J. Electron. Mater. 48 (2019) 6231–6239, https://doi.org/10.1007/s11664-019-07414-0.
[48] E.R. Khoder, H. Korri-Youssoufi, E-DNA biosensors of M. tuberculosis based on nanostructured polypyrrole, Mater. Sci. Eng. C 108 (2020) 110371.
[49] Y. Jiang, J. Wu, Recent development in chitosan nanocomposites for surface-based biosensor applications, Electrophoresis 40 (2019) 2084–2097, https://doi.org/10.1002/elps.201900066.
[50] A. Singh, G. Sinsinbar, M. Choudhary, V. Kumar, R. Pasricha, H.N. Verma, S. P. Singh, K. Arora, Graphene oxide-chitosan nanocomposite based electrochemical DNA biosensor for detection of typhoid, Sens. Actuat. B 185 (2013) 675–684, https://doi.org/10.1016/j.snb.2013.05.014.
[51] I. Tiwari, M. Singh, C.M. Pandey, G. Sumana, Electrochemical detection of a pathogenic *Escherichia coli* specific DNA sequence based on a graphene oxide-chitosan composite decorated with nickel ferrite nanoparticles, RSC Adv. 5 (2015) 67115–67124, https://doi.org/10.1039/c5ra07298k.
[52] S. Teixeira, N.S. Ferreira, R.S. Conlan, O.J. Guy, M.G.F. Sales, Chitosan/AuNPs modified graphene electrochemical sensor for label-free human chorionic gonadotropin detection, Electroanalysis 26 (2014) 2591–2598, https://doi.org/10.1002/elan.201400311.
[53] V.B. Juska, M.E. Pemble, A dual-enzyme, micro-band array biosensor based on the electrodeposition of carbon nanotubes embedded in chitosan and nanostructured Au-foams on microfabricated gold band electrodes, Analyst 145 (2020) 402–414, https://doi.org/10.1039/c9an01664c.
[54] L. Tian, J. Qi, X. Ma, X. Wang, C. Yao, W. Song, Y. Wang, A facile DNA strand displacement reaction sensing strategy of electrochemical biosensor based on N-carboxymethyl chitosan/molybdenum carbide nanocomposite for microRNA-21 detection, Biosens. Bioelectron. 122 (2018) 43–50, https://doi.org/10.1016/j.bios.2018.09.037.
[55] A. Coatrini-Soares, J.C. Soares, M. Popolin-Neto, S.S. de Mello, E.A. Sanches, F. V. Paulovich, O.N. Oliveira Jr, L.H.C. Mattoso, Multidimensional calibration spaces in Staphylococcus Aureus detection using chitosan-based genosensors and electronic tongue, Int. J. Biol. Macromol. 271 (2024) 132460, https://doi.org/10.1016/j.ijbiomac.2024.132460.
[56] A.M. Fernandes, M.H. Abdalhai, J. Ji, B.W. Xi, J. Xie, J. Sun, R. Noeline, B.H. Lee, X. Sun, Development of highly sensitive electrochemical genosensor based on multiwalled carbon nanotubes-chitosan-bismuth and lead sulfide nanoparticles for the detection of pathogenic Aeromonas, Biosens. Bioelectron. 63 (2015) 399–406, https://doi.org/10.1016/j.bios.2014.07.054.
[57] I. Tiwari, M. Singh, C.M. Pandey, G. Sumana, Electrochemical genosensor based on graphene oxide modified iron oxide–chitosan hybrid nanocomposite for pathogen detection, Sens. Actuat. B 206 (2015) 276–283, https://doi.org/10.1016/j.snb.2014.09.056.
[58] Z. Huang, C. Ge, S. Li, M. Cai, Y. Hui, X. Liao, Q. Zeng, Biomimetic pyrolytic MXene-based multifunctional films with multi-level structure for wearable piezoresistive devices and bioelectronics, Adv. Funct. Mater. 2422374 (2024) 1–14, https://doi.org/10.1002/adfm.202422374.
[59] K. Ketabi, H. Soleimanjahi, A. Teimoori, B. Hatamluyi, M. Rezayi, Z. Meshkat, Diagnostic genosensor for detection of rotavirus based on HFGNs/MXene/PPY signal amplification, Microchim. Acta 190 (2023), https://doi.org/10.1007/s00604-023-05871-3.
[60] J. Zhang, Y. Li, S. Duan, F. He, Highly electrically conductive two-dimensional Ti3C2 mxenes-based 16S rDNA electrochemical sensor for detecting mycobacterium tuberculosis, Anal. Chim. Acta 1123 (2020) 9–17, https://doi.org/10.1016/j.aca.2020.05.013.
[61] N. Shishegari, A. Tadjarodi, E. Omidinia, Talanta an electrochemical nano-genosensor for SARS-CoV-2 detection utilizing Ce-metal organic framework , dendritic palladium nano-structure , and sulfur-doped graphene oxide, Talanta 287 (2025) 127662, https://doi.org/10.1016/j.talanta.2025.127662.
[62] L. Huang, N. Yuan, W. Guo, Y. Zhang, W. Zhang, An electrochemical biosensor for the highly sensitive detection of Staphylococcus aureus based on SRCA-CRISPR/Cas12a, Talanta 252 (2022) 123821, https://doi.org/10.1016/j.talanta.2022.123821.
[63] Y. He, F. Jia, Y. Sun, W. Fang, Y. Li, J. Chen, Y. Fu, An electrochemical sensing method based on CRISPR/Cas12a system and hairpin DNA probe for rapid and sensitive detection of *Salmonella typhimurium*, Sens. Actuat. B 369 (2022) 132301, https://doi.org/10.1016/j.snb.2022.132301.
[64] C. Li, Y. Liang, Q. Feng, An electrochemical biosensor utilizing CRISPR/Cas12a amplification for the detection of *E. coli*, Anal. (2025) 1158–1166, https://doi.org/10.1039/d4an01441c.
[65] H.V. Nguyen, S. Hwang, S.W. Lee, E. Jin, M.H. Lee, Detection of HPV 16 and 18 L1 genes by a nucleic acid amplification-free electrochemical biosensor powered by CRISPR/Cas9, Bioelectrochemistry 162 (2025), https://doi.org/10.1016/j.bioelechem.2024.108861.
[66] T. Fan, S. Zhang, C. Meng, L. Gao, L. Yan, H. Wang, X. Shi, Y. Ge, H. Zhang, J. Hu, Ultrasensitive detection of nucleic acid with a CRISPR/Cas12a empowered electrochemical sensor based on antimonene, FlatChem 45 (2024), https://doi.org/10.1016/j.flatc.2024.100633.
[67] J. Wang, Q. Xia, J. Wu, Y. Lin, H. Ju, A sensitive electrochemical method for rapid detection of dengue virus by CRISPR/Cas13a-assisted catalytic hairpin assembly, Anal. Chim. Acta 1187 (2021), https://doi.org/10.1016/j.aca.2021.339131.
[68] C. Wu, Z. Chen, C. Li, Y. Hao, Y. Tang, Y. Yuan, L. Chai, T. Fan, J. Yu, X. Ma, O. A. Al-Hartomy, S. Wageh, A.G. Al-Sehemi, Z. Luo, Y. He, J. Li, Z. Xie, H. Zhang, CRISPR-Cas12a-empowered electrochemical biosensor for rapid and ultrasensitive detection of SARS-CoV-2 delta variant, Nano-Micro Lett. 14 (2022), https://doi.org/10.1007/s40820-022-00888-4.
[69] S. Barreda-Garcia, R. Miranda-Castro, N. de-los-Santos-Alvarez, M.J. Lobo-Castanon, Sequence-specific electrochemical detection of enzymatic amplification products of Salmonella genome on ITO electrodes improves pathogen detection to the single copy level, Sens. Actuat. B 268 (2018) 438–445, https://doi.org/10.1016/j.snb.2018.04.133.
[70] W. Jaroenram, J. Kampeera, N. Arunrut, C. Karuwan, A. Sappat, P. Khumwan, S. Jaitrong, K. Boonnak, T. Prammananan, A. Chaiprasert, A. Tuantranont, W. Kiatpathomchai, Graphene-based electrochemical genosensor incorporated loop-mediated isothermal amplification for rapid on-site detection of mycobacterium tuberculosis, J. Pharm. Biomed. Anal. 186 (2020) 113333, https://doi.org/10.1016/j.jpba.2020.113333.
[71] T. Notomi, H. Okayama, H. Masubuchi, T. Yonekawa, K. Watanabe, N. Amino, T. Hase, Loop-mediated isothermal amplification of DNA, Nucleic Acids Res. 28 (2000) e63, https://doi.org/10.1093/nar/28.12.e63.
[72] Q. Li, Y. Li, Q. Gao, C. Jiang, Q. Tian, C. Ma, C. Shi, Real-time monitoring of isothermal nucleic acid amplification on a smartphone by using a portable electrochemical device for home-testing of SARS-CoV-2: a portable device for home-testing of SARS-CoV-2 via the electrochemical method, Anal. Chim. Acta 1229 (2022) 340343, https://doi.org/10.1016/j.aca.2022.340343.
[73] K. Marchlewicz, I. Ostrowska, S. Oszwałdowski, A. Zasada, R. Ziolkowski, E. Malinowska, Molecular diagnostic of toxigenic Corynebacterium diphtheriae strain by DNA sensor potentially suitable for electrochemical point-of-care diagnostic, Talanta 227 (2021) 122161, https://doi.org/10.1016/j.talanta.2021.122161.
[74] Y. Ye, W. Yan, Y. Liu, S. He, X. Cao, X. Xu, H. Zheng, S. Gunasekaran, Electrochemical detection of Salmonella using an invA genosensor on polypyrrole-reduced graphene oxide modifi ed glassy carbon electrode and AuNPs-horseradish peroxidase-streptavidin as nanotag, Anal. Chim. Acta 1074 (2019) 80–88, https://doi.org/10.1016/j.aca.2019.05.012.
[75] A. Sappat, W. Jaroenram, T. Puthawibool, T. Lomas, A. Tuantranont, W. Kiatpathomchai, Detection of shrimp Taura syndrome virus by loop-mediated isothermal amplification using a designed portable multi-channel turbidimeter, J. Virol. Methods 175 (2011) 141–148, https://doi.org/10.1016/j.jviromet.2011.05.013.
[76] A. Ben Aissa, N. Madaboosi, M. Nilsson, M.I. Pividori, Electrochemical genosensing of *E. coli* based on padlock probes and rolling circle amplification, Sensors 21 (2021) 1749, https://doi.org/10.3390/s21051749.
[77] A. Mobed, M. Hasanzadeh, S. Hassanpour, A. Saadati, M. Agazadeh, A. Mokhtarzadeh, An innovative nucleic acid based biosensor toward detection of Legionella pneumophila using DNA immobilization and hybridization: a novel genosensor, Microchem. J. 148 (2019) 708–716, https://doi.org/10.1016/j.microc.2019.05.027.
[78] M.S. Bacchu, M.R. Ali, S. Das, S. Akter, H. Sakamoto, S.I. Suye, M.M. Rahman, K. Campbell, M.Z.H. Khan, A DNA functionalized advanced electrochemical biosensor for identification of the foodborne pathogen Salmonella enterica serovar Typhi in real samples, Anal. Chim. Acta 1192 (2022) 339332, https://doi.org/10.1016/j.aca.2021.339332.
[79] J. Li, J. Jiang, Y. Su, Y. Liang, C. Zhang, A novel cloth-based supersandwich electrochemical aptasensor for direct, sensitive detection of pathogens, Anal. Chim. Acta 1188 (2021) 339176, https://doi.org/10.1016/j.aca.2021.339176.
[80] E. Eksin, An electrochemical assay for sensitive detection of Acinetobacter baumannii gene, Talanta 249 (2022) 123696, https://doi.org/10.1016/j.talanta.2022.123696.
[81] K.S. Rizi, B. Hatamluyi, M. Darroudi, Z. Meshkat, E. Aryan, S. Soleimanpour, M. Rezayi, PCR-free electrochemical genosensor for Mycobacterium tuberculosis complex detection based on two-dimensional Ti3C2 Mxene-polypyrrole signal amplification, Microchem. J. 179 (2022) 107467, https://doi.org/10.1016/j.microc.2022.107467.
[82] L. Cheng, Y. He, Y. Yang, J. Chen, H. He, Y. Liu, Z. Lin, G. Hong, Highly reproducible and sensitive electrochemical biosensor for Chlamydia trachomatis detection based on duplex-specific nuclease-assisted target-responsive DNA hydrogels and bovine serum albumin carrier platform, Anal. Chim. Acta 1197 (2022) 339496, https://doi.org/10.1016/j.aca.2022.339496.
[83] J.M.R. Flauzino, R.C.S. Peres, L.M. Alves, J.G. Vieira, G. Julia, A.G. Brito-madurro, J.M. Madurro, DNA electrochemical biosensor for detection of alicyclobacillus acidoterrestris utilizing Hoechst 33258 as indicator, Bioelectrochemistry 140 (2021) 107801, https://doi.org/10.1016/j.bioelechem.2021.107801.
[84] F. Shi, B. Wang, L. Yan, B. Wang, Y. Niu, L. Wang, W. Sun, In-situ growth of nitrogen-doped carbonized polymer dots on black phosphorus for electrochemical DNA biosensor of *Escherichia coli* O157 : H7, Bioelectrochemistry 148 (2022) 108226, https://doi.org/10.1016/j.bioelechem.2022.108226.
[85] E.Y. Ariffin, Y.H. Lee, D. Futra, L.L. Tan, N. Huda, A. Karim, N. Nuraznida, N. Ibrahim, A. Ahmad, An ultrasensitive hollow-silica-based biosensor for pathogenic *Escherichia coli* DNA detection, Ana. Bioanal. Chem. (2018) 2363–2375.
[86] R. Nazari-Vanani, N. Sattarahmady, H. Yadegari, H. Heli, A novel and ultrasensitive electrochemical DNA biosensor based on an ice crystals-like gold nanostructure for the detection of Enterococcus faecalis gene sequence, Colloids Surf. B 166 (2018) 245–253, https://doi.org/10.1016/j.colsurfb.2018.03.025.
[87] R. Nazari-Vanani, N. Sattarahmady, H. Yadegari, M. Khatami, H. Heli, Electrochemical biosensing of 16s rRNA gene sequence of Enterococcus faecalis, Biosens. Bioelectron. 142 (2019) 111541, https://doi.org/10.1016/j.bios.2019.111541.

[88] A. Rahi, N. Sattarahmady, H. Heli, An ultrasensitive electrochemical genosensor for Brucella based on palladium nanoparticles, Anal. Biochem. 510 (2016) 11–17, https://doi.org/10.1016/j.ab.2016.07.012.
[89] A. Rahi, N. Sattarahmady, H. Heli, Zepto-molar electrochemical detection of Brucella genome based on gold nanoribbons covered by gold nanoblooms, Sci. Rep. 5 (2015) 18060, https://doi.org/10.1038/srep18060.
[90] N. Delshadi-Jahromi, R. Nazari-Vanani, H. Yadegari, N. Sattarahmady, G. R. Hatam, Label-free ultrasensitive electrochemical genosensing of Trichomonas vaginalis using anisotropic-shaped gold nanoparticles as a platform, a repeated sequence of the parasite DNA as a probe, and toluidine blue as a redo, Sens. Actuat. B 273 (2018) 234–241, https://doi.org/10.1016/j.snb.2018.06.051.
[91] R.Dehdari Vais, H. Heli, N. Sattarahmady, Label-free electrochemical DNA biosensing of MR TV 29 18s ribosomal RNA gene of Trichomonas vaginalis by signalization of non-spherical gold nanoparticles, Mater. Today Commun. 34 (2023) 105123, https://doi.org/10.1016/j.mtcomm.2022.105123.
[92] R.Dehdari Vais, H. Heli, N. Sattarahmady, A. Barazesh, A novel and ultrasensitive label-free electrochemical DNA biosensor for trichomonas vaginalis detection based on a nanostructured film of poly(ortho-aminophenol), Synth. Met. 287 (2022) 117082, https://doi.org/10.1016/j.synthmet.2022.117082.
[93] R. Nazari-Vanani, H. Heli, N. Sattarahmady, An impedimetric genosensor for Leishmania infantum based on electrodeposited cadmium sulfide nanosheets, Talanta 217 (2020) 121080, https://doi.org/10.1016/j.talanta.2020.121080.
[94] R. Nazari-Vanani, N. Sattarahmady, H. Yadegari, N. Delshadi, G.R. Hatam, H. Heli, Electrochemical quantitation of Leishmania infantum based on detection of its kDNA genome and transduction of non-spherical gold nanoparticles, Anal. Chim. Acta 1041 (2018) 40–49, https://doi.org/10.1016/j.aca.2018.08.036.
[95] N. Delshadi-Jahromi, R. Nazari-Vanani, H. Yadegari, N. Sattarahmady, G. R. Hatam, H. Heli, Label-free ultrasensitive electrochemical genosensing of Trichomonas vaginalis using anisotropic-shaped gold nanoparticles as a platform, a repeated sequence of the parasite DNA as a probe, and toluidine blue as a redox marker, Sens. Actuat. B 273 (2018) 234–241, https://doi.org/10.1016/j.snb.2018.06.051.
[96] M. Moradi, N. Sattarahmady, A. Rahi, G.R. Hatam, S.M.R. Sorkhabadi, H. Heli, A label-free, PCR-free and signal-on electrochemical DNA biosensor for Leishmania major based on gold nanoleaves, Talanta 161 (2016) 48–53, https://doi.org/10.1016/j.talanta.2016.08.030.
[97] M. Moradi, N. Sattarahmady, G.R. Hatam, H. Heli, Electrochemical genosensing of leishmania major using gold hierarchical nanoleaflets, J. Biol. Today's World 5 (2016) 128–136, https://doi.org/10.15412/J.JBTW.01050801.
[98] H. Heli, N. Sattarahmady, G.R. Hatam, F. Reisi, R.Dehdari Vais, An electrochemical genosensor for Leishmania major detection based on dual effect of immobilization and electrocatalysis of cobalt-zinc ferrite quantum dots, Talanta 156–157 (2016) 172–179, https://doi.org/10.1016/j.talanta.2016.04.065.
[99] Y.H. Liu, H.H. Deng, H.N. Li, T.F. Shi, H.P. Peng, A.L. Liu, W. Chen, G.L. Hong, A DNA electrochemical biosensor based on homogeneous hybridization for the determination of Cryptococcus neoformans, J. Electroanal. Chem. 827 (2018) 27–33, https://doi.org/10.1016/j.jelechem.2018.09.001.
[100] P.H.G. Guedes, G. Brussasco, A.C.R. Moço, D.D. Moraes, R. Flauzino, L.F.G. Luz, M.T.G. Almeida, M.M.C.N. Soares, R.J. Oliveira, M. Madurro, A.G. Brito-Madurro, Ninhydrin as a novel DNA hybridization indicator applied to a highly reusable electrochemical genosensor for Candida auris, Talanta 235 (2021) 122694, https://doi.org/10.1016/j.talanta.2021.122694.
[101] K. Rana, J. Mittal, J. Narang, A. Mishra, R.N. Pudake, Graphene based electrochemical DNA biosensor for detection of false smut of rice (Ustilaginoidea virens), Plant Pathol. J. 37 (2021) 291–298, https://doi.org/10.5423/PPJ.OA.11.2020.0207.
[102] I. Yahyavi, F. Edalat, N. Pirbonyeh, A. Letafati, N. Sattarahmady, H. Heli, A. Moattari, Nucleic acid-based electrochemical biosensor for detection of influenza B by gold nanoparticles, J. Mol. Recognit. 37 (2024) e3073, https://doi.org/10.1002/jmr.3073.
[103] J. Mohammadi, A. Moattari, N. Sattarahmady, N. Pirbonyeh, H. Yadegari, H. Heli, Electrochemical biosensing of influenza A subtype genome based on meso/macroporous cobalt (II) oxide nanoflakes-applied to human samples, Anal. Chim. Acta 979 (2017) 51–57, https://doi.org/10.1016/j.aca.2017.05.010.
[104] S. Lv, Y. Tang, K. Zhang, D. Tang, Wet NH3-triggered NH2-MIL-125(Ti) structural switch for visible fluorescence immunoassay impregnated on paper, Anal. Chem. 90 (2018) 14121–14125, https://doi.org/10.1021/acs.analchem.8b04981.
[105] Z. Qiu, J. Shu, D. Tang, Bioresponsive release system for visual fluorescence detection of carcinoembryonic antigen from mesoporous silica nanocontainers mediated optical color on quantum dot-enzyme-impregnated paper, Anal. Chem. 89 (2017) 5152–5160, https://doi.org/10.1021/acs.analchem.7b00989.
[106] S. Lv, K. Zhang, L. Zhu, D. Tang, R. Niessner, D. Knopp, H2-based electrochemical biosensor with Pd nanowires@ZIF-67 molecular sieve bilayered sensing interface for immunoassay, Anal. Chem. 91 (2019) 12055–12062, https://doi.org/10.1021/acs.analchem.9b03177.
[107] E. Pishbin, F. Sadri, A. Dehghan, M.J. Kiani, N. Hashemi, I. Zare, P. Mousavi, A. Rahi, Recent advances in isolation and detection of exosomal microRNAs related to Alzheimer's disease, Environ. Res. 227 (2023) 115705, https://doi.org/10.1016/j.envres.2023.115705.
[108] M.I.H. Ansari, S. Hassan, A. Qurashi, F.A. Khanday, Microfluidic-integrated DNA nanobiosensors, Biosens. Bioelectron. 85 (2016) 247–260, https://doi.org/10.1016/j.bios.2016.05.009.
[109] J. Kudr, O. Zitka, M. Klimanek, R. Vrba, V. Adam, Microfluidic electrochemical devices for pollution analysis-a review, Sens. Actuat. B 246 (2017) 578–590, https://doi.org/10.1016/j.snb.2017.02.052.
[110] J. Kim, M. Johnson, P. Hill, B.K. Gale, Microfluidic sample preparation: cell lysis and nucleic acid purification, Integr. Biol. 1 (2009) 574–586, https://doi.org/10.1039/b905844c.
[111] D. Obino, M. Vassalli, A. Franceschi, A. Alessandrini, P. Facci, F. Viti, An overview on microfluidic systems for nucleic acids extraction from human raw samples, Sensors 21 (2021) 3058, https://doi.org/10.3390/s21093058.
[112] M.S. Islam, A. Aryasomayajula, P.R. Selvaganapathy, A review on macroscale and microscale cell lysis methods, Micromachines 8 (2017) 83, https://doi.org/10.3390/mi8030083.
[113] R. Kotlowski, A. Martin, A. Ablordey, K. Chemlal, P.A. Fonteyne, F. Portaels, One-tube cell lysis and DNA extraction procedure for PCR-based detection of Mycobacterium ulcerans in aquatic insects, molluscs and fish, J. Med. Microbiol. 53 (2004) 927–933, https://doi.org/10.1099/jmm.0.45593-0.
[114] R. Fradique, A.M. Azevedo, V. Chu, J.P. Conde, M.R. Aires-Barros, Microfluidic platform for rapid screening of bacterial cell lysis, J. Chromatogr. A. 1610 (2020) 460539, https://doi.org/10.1016/j.chroma.2019.460539.
[115] R. Sharma, B.D. Dill, K. Chourey, M. Shah, N.C. Verberkmoes, R.L. Hettich, Coupling a detergent lysis/cleanup methodology with intact protein fractionation for enhanced proteome characterization, J. Proteome Res. 11 (2012) 6008–6018, https://doi.org/10.1021/pr300709k.
[116] R.B. Brown, J. Audet, Current techniques for single-cell lysis, J. R. Soc. Interface 5 (2008) S131–S138, https://doi.org/10.1098/rsif.2008.0009.focus.
[117] K. Ward, Z.H. Fan, Mixing in microfluidic devices and enhancement methods, J. Micromech. Microeng. 25 (2015) 094001, https://doi.org/10.1088/0960-1317/25/9/094001.
[118] L. Gorgannezhad, H. Stratton, N.T. Nguyen, Microfluidic-based nucleic acid amplification systems in microbiology, Micromachines 10 (2019) 408, https://doi.org/10.3390/mi10060408.
[119] C.Y. Lee, G. Bin Lee, J.L. Lin, F.C. Huang, C.S. Liao, Integrated microfluidic systems for cell lysis, mixing/pumping and DNA amplification, J. Micromech. Microeng. 15 (2005) 1215–1223, https://doi.org/10.1088/0960-1317/15/6/011.
[120] M.M. Packard, E.K. Wheeler, E.C. Alocilja, M. Shusteff, Performance evaluation of fast microfluidic thermal lysis of bacteria for diagnostic sample preparation, Diagnostics 3 (2013) 105–116, https://doi.org/10.3390/diagnostics3010105.
[121] F. Jiang, J. Chen, J. Yu, Design and application of a microfluidic cell lysis microelectrode chip, Instrum. Sci. Technol. 44 (2016) 223–232, https://doi.org/10.1080/10739149.2015.1076839.
[122] T. Geng, C. Lu, Microfluidic electroporation for cellular analysis and delivery, Lab Chip 13 (2013) 3803–3821, https://doi.org/10.1039/c3lc50566a.
[123] K. Pandian, M. Ajanth Praveen, S.Z. Hoque, A. Sudeepthi, A.K. Sen, Continuous electrical lysis of cancer cells in a microfluidic device with passivated interdigitated electrodes, Biomicrofluidics 14 (2020) 064101, https://doi.org/10.1063/5.0026046.
[124] H. Sedgwick, F. Caron, P.B. Monaghan, W. Kolch, J.M. Cooper, Lab-on-a-chip technologies for proteomic analysis from isolated cells, J. R. Soc. Interface 5 (2008) S123–S130, https://doi.org/10.1098/rsif.2008.0169.focus.
[125] M.S. Islam, K. Kuryllo, P.R. Selvaganapathy, Y. Li, M.J. Deen, A microfluidic sample preparation device for pre-concentration and cell lysis using a nanoporous membrane, in: 17th Int. Conf. Miniaturized Syst. Chem. Life Sci. MicroTAS 2013, 2013, pp. 1105–1107.
[126] H. Jeon, S. Kim, G. Lim, Electrical force-based continuous cell lysis and sample separation techniques for development of integrated microfluidic cell analysis system: a review, Microelectron. Eng. 198 (2018) 55–72, https://doi.org/10.1016/j.mee.2018.06.010.
[127] G. Mernier, N. Piacentini, T. Braschler, N. Demierre, P. Renaud, Continuous-flow electrical lysis device with integrated control by dielectrophoretic cell sorting, Lab Chip 10 (2010) 2077–2082, https://doi.org/10.1039/c000977f.
[128] R. Ziv, Y. Steinhardt, G. Pelled, D. Gazit, B. Rubinsky, Micro-electroporation of mesenchymal stem cells with alternating electrical current pulses, Biomed. Microdevices 11 (2009) 95–101, https://doi.org/10.1007/s10544-008-9213-4.
[129] K.K. Sang, H.K. Jae, P.K. Kwang, D.C. Taek, Continuous low-voltage de electroporation on a microfluidic chip with polyelectrolytic salt bridges, Anal. Chem. 79 (2007) 7761–7766, https://doi.org/10.1021/ac071197h.
[130] X.Y. Wei, J.H. Li, L. Wang, F. Yang, Low-voltage electrical cell lysis using a microfluidic device, Biomed. Microdevices 21 (2019) 22, https://doi.org/10.1007/s10544-019-0369-x.
[131] Y.J. Lo, U. Lei, A continuous flow-through microfluidic device for electrical lysis of cells, Micromachines 10 (2019) 247, https://doi.org/10.3390/mi10040247.
[132] A. Olanrewaju, M. Beaugrand, M. Yafia, D. Juncker, Capillary microfluidics in microchannels: from microfluidic networks to capillaric circuits, Lab Chip 18 (2018) 2323–2347, https://doi.org/10.1039/c8lc00458g.
[133] A. Dehghan, A. Gholizadeh, M. Navidbakhsh, H. Sadeghi, E. Pishbin, Integrated microfluidic system for efficient DNA extraction using on-disk magnetic stirrer micromixer, Sens. Actuat. B 351 (2022) 130919, https://doi.org/10.1016/j.snb.2021.130919.
[134] H. Kido, M. Micic, D. Smith, J. Zoval, J. Norton, M. Madou, A novel, compact disk-like centrifugal microfluidics system for cell lysis and sample homogenization, Colloids Surf. B 58 (2007) 44–51, https://doi.org/10.1016/j.colsurfb.2007.03.015.
[135] T.C. Marentis, B. Kusler, G.G. Yaralioglu, S. Liu, E.O. Hæggstrom, B.T. Khuri-Yakub, Microfluidic sonicator for real-time disruption of eukaryotic cells and bacterial spores for DNA analysis, Ultrasound Med. Biol. 31 (2005) 1265–1277, https://doi.org/10.1016/j.ultrasmedbio.2005.05.005.

[136] D. Di Carlo, K.H. Jeong, L.P. Lee, Reagentless mechanical cell lysis by nanoscale barbs in microchannels for sample preparation, Lab Chip 3 (2003) 287–291, https://doi.org/10.1039/b305162e.
[137] J.Y. Han, M. Wiederoder, D.L. DeVoe, Isolation of intact bacteria from blood by selective cell lysis in a microfluidic porous silica monolith, Microsyst. Nanoeng. 5 (2019) 30, https://doi.org/10.1038/s41378-019-0063-4.
[138] L. Xia, G. Li, Recent progress of microfluidics in surface-enhanced raman spectroscopic analysis, J. Sep. Sci. 44 (2021) 1752–1768, https://doi.org/10.1002/jssc.202001196.
[139] L. Xia, G. Li, Recent progress of microfluidic sample preparation techniques, J. Sep. Sci. 46 (2023) e2300327, https://doi.org/10.1002/jssc.202300327.
[140] J.F. Hess, M.E. Hess, R. Zengerle, N. Paust, M. Boerries, T. Hutzenlaub, Automated library preparation for whole genome sequencing by centrifugal microfluidics, Anal. Chim. Acta 1182 (2021) 338954, https://doi.org/10.1016/j.aca.2021.338954.
[141] W. Ouyang, J. Han, One-step nucleic acid purification and noise-resistant polymerase chain reaction by electrokinetic concentration for ultralow-abundance nucleic acid detection, Angew. Chemie 59 (2020) 10981–10988, https://doi.org/10.1002/anie.201915788.
[142] A.J. Conde, I. Keraite, A.E. Ongaro, M. Kersaudy-Kerhoas, Versatile hybrid acoustic micromixer with demonstration of circulating cell-free DNA extraction from sub-ml plasma samples, Lab Chip 20 (2020) 741–748, https://doi.org/10.1039/c9lc01130g.
[143] J. Yin, Z. Zou, Z. Hu, S. Zhang, F. Zhang, B. Wang, S. Lv, Y. Mu, A "sample-in-multiplex-digital-answer-out" chip for fast detection of pathogens, Lab Chip 20 (2020) 979–986, https://doi.org/10.1039/c9lc01143a.
[144] K. Lee, A. Tripathi, Parallel DNA extraction from whole blood for rapid sample generation in genetic epidemiological studies, Front. Genet. 11 (2020) 374, https://doi.org/10.3389/fgene.2020.00374.
[145] A.T. Abafogi, J. Kim, J. Lee, M.O. Mohammed, D. van Noort, S. Park, 3D-printed modular microfluidic device enabling preconcentrating bacteria and purifying bacterial DNA in blood for improving the sensitivity of molecular diagnostics, Sensors 20 (2020) 1202, https://doi.org/10.3390/s20041202.
[146] S. Kwon, J. Oh, M.S. Lee, E. Um, J. Jeong, J.H. Kang, Enhanced diamagnetic repulsion of blood cells enables versatile plasma separation for biomarker analysis in blood, Small 17 (2021) e2100797, https://doi.org/10.1002/smll.202100797.
[147] A. Jagannath, Y. Li, H. Cong, J. Hassan, G. Gonzalez, W. Wang, N. Zhang, M. D. Gilchrist, UV-assisted hyperbranched poly(β-amino ester) modification of a silica membrane for two-step microfluidic dna extraction from blood, ACS Appl. Mater. Interfaces 15 (2023) 31159–31172, https://doi.org/10.1021/acsami.3c03523.
[148] H. Lee, C. Park, W. Na, K.H. Park, S. Shin, Precision cell-free DNA extraction for liquid biopsy by integrated microfluidics, NPJ Precis. Oncol. 4 (2020) 3, https://doi.org/10.1038/s41698-019-0107-0.
[149] L.T.H. Thang, W. Han, J. Shin, J.H. Shin, Disposable, pressure-driven, and self-contained cartridge with pre-stored reagents for automated nucleic acid extraction, Sens. Actuat. B 375 (2023) 132948, https://doi.org/10.1016/j.snb.2022.132948.
[150] S. Berensmeier, Magnetic particles for the separation and purification of nucleic acids, Appl. Microbiol. Biotechnol. 73 (2006) 495–504, https://doi.org/10.1007/s00253-006-0675-0.
[151] S.M. Azimi, G. Nixon, J. Ahern, W. Balachandran, A magnetic bead-based DNA extraction and purification microfluidic device, Microfluid. Nanofluid. 11 (2011) 157–165, https://doi.org/10.1007/s10404-011-0782-9.
[152] Y. Wang, W. Qi, L. Wang, J. Lin, Y. Liu, Magnetic bead chain-based continuous-flow dna extraction for microfluidic pcr detection of salmonella, Micromachines 12 (2021) 384, https://doi.org/10.3390/mi12040384.
[153] H.G. Kye, C.D. Ahrberg, B.S. Park, J.M. Lee, B.G. Chung, Separation, purification, and detection of cfDNA in a microfluidic device, Biochip J. 14 (2020) 195–203, https://doi.org/10.1007/s13206-020-4208-1.
[154] C.H. Kim, J. Park, S.J. Kim, D.H. Ko, S.H. Lee, S.J. Lee, J.K. Park, M.K. Lee, On-site extraction and purification of bacterial nucleic acids from blood samples using an unpowered microfluidic device, Sens. Actuat. B 320 (2020) 128346, https://doi.org/10.1016/j.snb.2020.128346.
[155] H. Ben-Yoav, P.H. Dykstra, W.E. Bentley, R. Ghodssi, A controlled microfluidic electrochemical lab-on-a-chip for label-free diffusion-restricted DNA hybridization analysis, Biosens. Bioelectron. 64 (2015) 579–585, https://doi.org/10.1016/j.bios.2014.09.069.
[156] A. Thiha, F. Ibrahim, S. Muniandy, I.J. Dinshaw, S.J. Teh, K.L. Thong, B.F. Leo, M. Madou, All-carbon suspended nanowire sensors as a rapid highly-sensitive label-free chemiresistive biosensing platform, Biosens. Bioelectron. 107 (2018) 145–152, https://doi.org/10.1016/j.bios.2018.02.024.
[157] N. Duan, B. Xu, S. Wu, Z. Wang, Magnetic nanoparticles-based aptasensor using gold nanoparticles as colorimetric probes for the detection of *Salmonella typhimurium*, Anal. Sci. 32 (2016) 431–436, https://doi.org/10.2116/analsci.32.431.
[158] E.K. Sackmann, A.L. Fulton, D.J. Beebe, The present and future role of microfluidics in biomedical research, Nature 507 (2014) 181–189, https://doi.org/10.1038/nature13118.
[159] P.S. Sfragano, E.C. Reynoso, N.E. Rojas-Ruíz, S. Laschi, G. Rossi, M. Buchinger, E. Torres, I. Palchetti, A microfluidic card-based electrochemical assay for the detection of sulfonamide resistance genes, Talanta 271 (2024) 125718, https://doi.org/10.1016/j.talanta.2024.125718.
[160] P. Parthasarathy, M. Venkatesh, Developments in microfluidic integrated lab-on-chip devices for DNA biosensing towards unifying the emergence of nanobiosensor, Biomed. Mater. Devices (2024), https://doi.org/10.1007/s44174-024-00257-2.
[161] A. Abouhagger, R. Celiešiūtė-Germanienė, N. Bakute, A. Stirke, W.C.M.A. Melo, Electrochemical biosensors on microfluidic chips as promising tools to study microbial biofilms: a review, Front. Cell. Infect. Microbiol. 14 (2024) 1419570, https://doi.org/10.3389/fcimb.2024.1419570.
[162] A.A. Akhlaghi, H. Kaur, B.R. Adhikari, L. Soleymani, Editors' choice—challenges and opportunities for developing electrochemical biosensors with commercialization potential in the point-of-care diagnostics market, ECS Sens. Plus 3 (2024), https://doi.org/10.1149/2754-2726/ad304a.
[163] S. Devrani, D. Tietze, A.A. Tietze, Automated microfluidic platform for high-throughput biosensor development, 2400116 (2025) 1–20. https://doi.org/10.1002/adsr.202400116.
[164] T. Zhang, X. Dong, X. Gao, Y. Yang, W. Song, J. Song, H. Bi, Y. Guo, J. Song, Applications of metals and metal compounds in improving the sensitivity of microfluidic biosensors – a review, Chem. - A Eur. J. 30 (2024), https://doi.org/10.1002/chem.202400578.
[165] S.L. Tsai, J.J. Wey, S.C. Lai, Y.Y. Huang, A novel microfluidic chip based on an impedance-enhanced electrochemical immunoassay, Phys. Fluids 37 (2025), https://doi.org/10.1063/5.0251565.
[166] Y.H. Cheng, R. Kargupta, D. Ghoshal, Z. Li, C. Chande, L. Feng, S. Chatterjee, N. Koratkar, R.K. Motkuri, S. Basuray, ESSENCE - a rapid, shear-enhanced, flow-through, capacitive electrochemical platform for rapid detection of biomolecules, Biosens. Bioelectron. 182 (2021) 113163, https://doi.org/10.1016/j.bios.2021.113163.
[167] S. Khaliliazar, I. Oberg Mansson, A. Piper, L. Ouyang, P. Reu, M.M. Hamedi, Woven electroanalytical biosensor for nucleic acid amplification tests, Adv. Healthc. Mater. 10 (2021) e2100034, https://doi.org/10.1002/adhm.202100034.
[168] D. Najjar, J. Rainbow, S. Sharma Timilsina, P. Jolly, H. de Puig, M. Yafia, N. Durr, H. Sallum, G. Alter, J.Z. Li, X.G. Yu, D.R. Walt, J.A. Paradiso, P. Estrela, J. J. Collins, D.E. Ingber, A lab-on-a-chip for the concurrent electrochemical detection of SARS-CoV-2 RNA and anti-SARS-CoV-2 antibodies in saliva and plasma, Nat. Biomed. Eng. 6 (2022) 968–978, https://doi.org/10.1038/s41551-022-00919-w.
[169] Y.M. Park, S.Y. Lim, S.J. Shin, C.H. Kim, S.W. Jeong, S.Y. Shin, N.H. Bae, S.J. Lee, J. Na, G.Y. Jung, T.J. Lee, A film-based integrated chip for gene amplification and electrochemical detection of pathogens causing foodborne illnesses, Anal. Chim. Acta 1027 (2018) 57–66, https://doi.org/10.1016/j.aca.2018.03.061.
[170] R. Chand, S. Ramalingam, S. Neethirajan, A 2D transition-metal dichalcogenide MoS2 based novel nanocomposite and nanocarrier for multiplex miRNA detection, Nanoscale 10 (2018) 8217–8225, https://doi.org/10.1039/c8nr00697k.
[171] F. Keyvani, N. Debnath, M. Ayman Saleh, M. Poudineh, An integrated microfluidic electrochemical assay for cervical cancer detection at point-of-care testing, Nanoscale 14 (2022) 6761–6770, https://doi.org/10.1039/d1nr08252c.
[172] L.M. Fu, Y.N. Wang, Detection methods and applications of microfluidic paper-based analytical devices, TrAC Trends Anal. Chem. 107 (2018) 196–211, https://doi.org/10.1016/j.trac.2018.08.018.
[173] M. Moccia, V. Caratelli, S. Cinti, B. Pede, C. Avitabile, M. Saviano, A.L. Imbriani, D. Moscone, F. Arduini, Paper-based electrochemical peptide nucleic acid (PNA) biosensor for detection of miRNA-492: a pancreatic ductal adenocarcinoma biomarker, Biosens. Bioelectron. 165 (2020) 112371, https://doi.org/10.1016/j.bios.2020.112371.
[174] X. Sun, H. Wang, Y. Jian, F. Lan, L. Zhang, H. Liu, S. Ge, J. Yu, Ultrasensitive microfluidic paper-based electrochemical/visual biosensor based on spherical-like cerium dioxide catalyst for miR-21 detection, Biosens. Bioelectron. 105 (2018) 218–225, https://doi.org/10.1016/j.bios.2018.01.025.
[175] C. Srisomwat, A. Yakoh, N. Chuaypen, P. Tangkijvanich, T. Vilaivan, O. Chailapakul, Amplification-free DNA sensor for the one-step detection of the hepatitis B Virus using an automated paper-based lateral flow electrochemical device, Anal. Chem. 93 (2021) 2879–2887, https://doi.org/10.1021/acs.analchem.0c04283.
[176] H. Ben-Yoav, P.H. Dykstra, W.E. Bentley, R. Ghodssi, A microfluidic-based electrochemical biochip for label-free diffusion-restricted DNA hybridization analysis, Biosens. Bioelectron. 38 (2012) 114–120, https://doi.org/10.1016/j.bios.2012.05.009.
[177] H. Kutluk, R. Bruch, G.A. Urban, C. Dincer, Impact of assay format on miRNA sensing: electrochemical microfluidic biosensor for miRNA-197 detection, Biosens. Bioelectron. 148 (2020) 111824, https://doi.org/10.1016/j.bios.2019.111824.
[178] M.J.A. Shiddiky, Y.B. Shim, Trace analysis of DNA: preconcentration, separation, and electrochemical detection in microchip electrophoresis using Au nanoparticles, Anal. Chem. 79 (2007) 3724–3733, https://doi.org/10.1021/ac0701177.
[179] B. Bhushan (Ed.), Springer Handbook of Nanotechnology, Springer, 2010.
[180] www.globalpointofcare.abbott/us/en/product-details/apoc/i-stat-system-us.html.
[181] medicalonex.com/nanomix-inc-29505/product/nanmix-elabr-analyzer/.
[182] www.appropedia.org/Daktari_CD4.
[183] kypha.net/products.htm#rapiplex.
[184] A.A. Zainuddin, A.F.M. Mansor, R.A. Rahim, A.N. Nordin, Optimization of printing techniques for electrochemical biosensors, in: AIP Conf. Proc., 2017, https://doi.org/10.1063/1.4975299.

[185] A. Hussain, N. Abbas, A. Ali, Inkjet printing: a viable technology for biosensor fabrication, Chemosensors 10 (2022), https://doi.org/10.3390/chemosensors10030103.
[186] K. Gavina, L.C. Franco, H. Khan, J.P. Lavik, R.F. Relich, Molecular point-of-care devices for the diagnosis of infectious diseases in resource-limited settings – A review of the current landscape, technical challenges, and clinical impact, J. Clin. Virol. 169 (2023), https://doi.org/10.1016/j.jcv.2023.105613.
[187] D. Vijian, S.V. Chinni, L.S. Yin, B. Lertanantawong, W. Surareungchai, Non-protein coding RNA-based genosensor with quantum dots as electrochemical labels for attomolar detection of multiple pathogens, Biosens. Bioelectron. 77 (2016) 805–811, https://doi.org/10.1016/j.bios.2015.10.057.
[188] L. Chen, D. Chen, M. Lian, Progress in the development of antifouling electrochemical biosensors, Curr. Anal. Chem. 20 (2024), https://doi.org/10.2174/0115734110320891240823065902.